Privatdoz. Dipl.-Ing. Dr.techn. Andreas Limbeck

TECHNISCHE UNIVERSITÄT WIEN
Vienna University of Technology

Diplomarbeit

„Elemental imaging using LA-ICP-MS on biological samples"

Ausgeführt am Institut für
Chemische Technologien und Analytik
der Technischen Universität Wien

Unter der Anleitung von
Privatdoz. Dipl.-Ing. Dr.techn. Andreas Limbeck

durch
Maximilian Bonta, BSc
Alser Straße 10/2/2/24
1090 Wien

Wien, am 30.7.2013

Maximilian Bonta, BSc

STAATSANWALT […] Madame kennen Santorin?

ELSA Santorin?

STAATSANWALT […] Eine Stadt wie aus Kreide, so weiß, so grell, emporgetürmt in den Wind und ins Licht, einsam und frei, emporgetürmt in einen Himmel ohne Dunst, ohne Dämmerung, ohne Hoffnung auf Jenseits, ringsum das Meer, nichts als die blaue Finsternis des Meeres…

ELSA Und da wollen Sie hin?

INGE Da wollen wir hin.

ELSA Und was wollen Sie dort machen?

STAATSANWALT – leben, Madame. Ohne Dämmerung, ohne Hoffnung auf ein andermal, alles ist jetzt, der Tag und die Nacht, das Meer, hier sind unsre Götter geboren, die wirklichen, hier sind sie aus den Fluten gestiegen, Kinder der Freude, Kinder des Lichts!

Max Frisch, Graf Öderland

Abstract

LA-ICP-MS imaging experiments are of growing interest within the field of biosciences. Revealing the distributions of major components as well as trace elements in biological samples can help to understand fundamental biological processes. However, obtaining accurate images and reliable quantitative information is in most cases a sophisticated task and requires properly developed methods. Measurement methods employed in the past only offer partly satisfactory results with several points of criticism. Highly variable sample conditions and changing instrumental parameters during measurement time aggravate even obtaining reliable qualitative information when measuring biological tissues. Despite ICP-MS is a quantitative mass spectrometric method most of the reported experiments only delivered qualitative information about the analyte distributions.

Especially investigations on the spatial distribution of trace elements in biosamples require an internal standard to compensate measurement artifacts. Both variations in the material desorption by the laser and changes of plasma conditions and detection sensitivity during measurement have to be monitored and eliminated by this internal standard having a constant distribution across the sample surface. Appearing instrumental drifts during measurement time and matrix related ablation differences can be compensated employing elaborate concepts for internal standardization. Furthermore the factor of day-to-day comparability of the performed experiments can be earned being an important point when measurements have to be performed in several parts or different samples should be compared.

When quantification is reported in literature matrix-matched standards have been utilized for quantification. For this method a tissue homogenate is spiked with a known amount of analyte, the tissue is brought to a solid form again and thin-slices are cut from the standard in the same way as from the sample material. So, this artificially created standard can be used for calibration. However, the use of matrix-matched standards has several limitations. By the development of novel standardization strategies these limitation should be overcome and the reliability of the obtained quantitative information will be increased. The use of appropriate internal standards facilitates the preparation of calibrations even without the utilization of matrix-matched standards.

In this work the development of an accurate internal standardization method using an inkjet pattern on different organic matrices is described, being a suitable alternative for the analysis of biological samples for testing of the internal standardization method. The spatial distribution of copper (from blue printing ink) is known due to the controlled printing process, other elements show homogenous distribution over the measured area. By the reduction of the monitored analytes and diminishing the complexity of the sample the amount of acquired data is reduced. These conditions ease the method development and evaluation before application to biological samples with unknown trace element concentrations.

The use of deposited gold thin-layers as an internal standard is evaluated and compared to measurements without an internal standard and with carbon as internal standard being often described and used in literature. Furthermore the homogeneity of the gold application is monitored to emphasize the usability of gold layers for signal normalization and quantification.

The actual amounts of copper could be easily determined by mineralization of the printed patterns and liquid ICP-MS measurement. High reproducibility of the printing process ensures that the copper amounts on all samples are only within a minor variance.

The results of this work underline the fact that gold layers with thicknesses in the nanometer range are a powerful tool for signal normalization in imaging LA-ICP-MS experiments. It could be shown that the gold deposition is homogenous and that normalization to the gold signal can compensate for variances in the experimental conditions such as instrumental drifts or matrix dependent changes in material ablation. The image quality could be drastically increased by reducing the standard deviation of the measurements and by compensating for matrix dependent ablation differences. Different sample matrices showed changed absolute analyte signals. This effect could be eliminated by the gold standardization. Furthermore a reliable method for signal quantification in LA-ICP-MS imaging experiments was developed. Using gold normalization it was possible to quantitatively determine elemental concentrations on unknown samples; the printed patterns were used as calibrations.

Kurzfassung

Die Darstellung der Verteilung (*Imaging*) von Heteroelementen auf biologischen Proben (meist Gewebeschnitte) mittels *laser ablation inductively coupled plasma mass spectrometry* (LA-ICP-MS) stellt ein immer wichtiger werdendes Gebiet im Bereich der Biowissenschaften dar. Die Kenntnis der Verteilung von Hauptkomponenten wie auch von Spurenelementen kann dazu beitragen, fundamentale biologische Prozesse näher zu verstehen. Problematische Punkte bei der Messung von Elementen auf biologischen Proben sind stark schwankende Probenbedingungen und sich verändernde instrumentelle Parameter während der Messzeit. Selbst bei Untersuchungen rein qualitativer Natur sind zahlreiche Limitationen zu berücksichtigen. Obwohl ICP-MS eine quantitative massenspektrometrische Methode ist, werden in der Literatur hauptsächlich qualitative Verteilungsbilder präsentiert.

Besonders für Untersuchungen der lateralen Verteilung von Elementen auf biologischen Proben wird ein interner Standard benötigt, um Artefakte in den erstellten Verteilungsbildern zu vermeiden. Sowohl Änderungen im Materialabtrag durch den Laser als auch sich verändernde Plasmabedingungen und Sensitivität des Detektors während der Messung sollten durch diesen internen Standard eliminiert werden. Dabei ist die gleichmäßige Verteilung des internen Standards über die Probenoberfläche ein wichtiger Faktor. Während der Messung auftretende instrumentelle Drifts und durch Änderungen der Matrix bedingte Unterschiede im Materialabtrag können durch die Verwendung geeigneter Konzepte zur Signalnormalisierung kompensiert werden. Ein weiterer Punkt, der sich durch die Verwendung von internen Standards ergibt ist eine Vergleichbarkeit von Proben, die an unterschiedlichen Tagen gemessen wurden.

Zur Quantifizierung in LA-ICP-MS *Imaging*-Experimenten wird in der Literatur am häufigsten die Verwendung von „matrix-angepassten“ Standards (*matrix-matched*) beschrieben. Hierbei wird ein Gewebehomogenat mit einer bekannten Menge an Analyt versetzt, wieder in feste Form gebracht und danach werden – wie von der Probe auch – Dünnschnitte angefertigt. Diese künstlich erzeugten Standards können nun zur Kalibration verwendet werden. Jedoch ergeben sich aus der Verwendung eben solcher Standards zahlreiche Einschränkungen. Durch die Entwicklung neuer Quantifizierungsstrategien sollen die vorhandenen Probleme eliminiert und gleichzeitig die Vertrauenswürdigkeit der erhaltenen Ergebnisse erhöht werden. Die Verwendung

von geeigneten internen Standards ermöglicht die Erstellung von Kalibrationen ohne *matrix-matched* Standards.

In der vorliegenden Arbeit wird eine Methode zur internen Standardisierung in LA-ICP-MS *Imaging*-Experimenten vorgestellt. Muster, die mit konventionellen Tintenstrahldruckern auf organische Matrices (z. B. normales Papier) geduckt werden, werden als Ersatz zu biologischen Proben zur Entwicklung und zum Testen von Standardisierungsmethoden verwendet. Das untersuchte Element ist Kupfer (in blauer Druckerfarbe enthalten), dessen Verteilung durch den kontrollierten Druckprozess bekannt ist. Alle anderen Elemente zeigen konstante Verteilung über die gesamte Probe. Durch die Reduktion der betrachteten Analyten und die Minimierung der Probenkomplexität kann die gesammelte Datenmenge auf ein übersichtliches Maß reduziert werden. Diese Bedingungen erleichtern die Methodenentwicklung und -evaluierung vor der Anwendung auf reale biologische Proben mit unbekannten Analytgehalten.

Die Verwendung von dünnen Goldschichten als internen Standard wurde evaluiert und mit Messungen ohne internen Standard und mit Kohlenstoff (in der Literatur häufig verwendet) als Standard verglichen. Weiters wurde die Homogenität der aufgebrachten Goldschichten untersucht, um das Einbringen möglicher Artefakte durch inhomogene Goldschichten zu vermeiden.

Die tatsächlichen Kupferkonzentrationen auf den Proben konnten leicht durch einen Säureaufschluss der geduckten Muster und anschließende ICP-MS Messung der Proben bestimmt werden. Die hohe Reproduzierbarkeit des Druckvorgangs stellt sicher, dass die Mengen an aufgebrachtem Kupfer innerhalb einer vernachlässigbaren Varianz liegen.

Die Ergebnisse der präsentierten Arbeit unterstreichen die Tatsache, dass Goldschichten mit Dicken im Nanometerbereich ein geeignetes Hilfsmittel zur Signalnormalisierung in LA-ICP-MS *Imaging*-Experimenten sind. Es konnte gezeigt werden, dass die Abscheidung der Goldschichten homogen ist und, dass die Normalisierung auf das Goldsignal die eine Eliminierung von instrumentellen Drifts und matrixabhängigen Ablationsunterschieden ermöglicht. Durch eine Reduktion der Standardabweichung der Messungen nach der Gold-Normalisierung konnte die Verlässlichkeit der erhaltenen *Images* gesteigert werden. Ohne Standardisierung ergaben sich auf unterschiedlichen

Matrices veränderte absolute Analytsignale. Durch Standardisierung auf das Goldsignal konnten diese Unterschiede eliminiert werden. Des Weiteren konnte eine verlässliche Quantifizierungsmethode für LA-ICP-MS *Imaging*-Experimente entwickelt werden. Es war möglich, quantitative Informationen über Analytverteilungen auf unbekannten Proben zu erhalten. Dabei können die Druckmuster als Kalibration verwendet werden.

Table of contents

Acknowledgment

Not only during my Master's thesis but throughout the last five years at Vienna University of Technology my life has been enriched and inspired by a variety of people. Hereby I want to address my gratitude to those who influenced me and my life during this time and were not only colleagues but also friends.

First I want to thank my supervisor Andreas Limbeck for giving me the possibility to work in his group and to conduct my Master's thesis. His support and countless fruitful discussions contributed in a great way to the results of the present work.

I have to express my special gratitude to Hans Lohninger for software development without that my work would not have proceeded that fast.

I want to thank all members of our working group for great working climate and for having a great time together.

Furthermore I want to thank my fellow students and friends. Some of them should be mentioned by their names, however completeness of the list cannot be guaranteed and those who are not named here will know that I am also grateful for their support. Thanks to Elke Ludwig, Michaela Helmel, Sandra Stranzinger and Max Kosok as well as Anja Cakara, Melanie Grandits and Melanie Feichter for having a great time together at the university and beyond. Also thanks to my other friends, namely Katja Staudigl, Nicole Rostok, Albrecht Reimer and Florian Karall as well as Carolina Vogel and Matthias and Philipp Heytmanek for being a major part of my life.

Last but not least I want to thank my parents for always supporting me morally and for always being there for me.

1. Introduction

ICP-MS is a method not only present in inorganic trace analysis but has also found its way into biochemical and biomedical analytics [1]. The ease of use combined with the high dynamic range and the capability of ultra-trace analysis makes ICP-MS a worthwhile method for a large number of applications. Especially employed in the field of proteomics [2-4] and immunochemistry [5] the described technique has for instance also been used for the analysis of trace metals in blood [6].

With the coupling of ICP-MS and laser ablation a powerful tool for solid sampling analysis with preservation of spatial distribution has been developed. The depiction of analyte distributions on biological surfaces (bio-imaging) is a topic of emerging interest in life sciences. Elemental imaging using LA-ICP-MS [7-9] is employed in a growing number of experiments [10] besides techniques capable of the analysis of molecular species (for example MALDI, IR, and SIMS) [11-15]. The capability of elemental analysis of non-metallic species and metalloids as well as trace metals appearing either in free form or bound to specific proteins [16, 17] makes LA-ICP-MS a versatile method for the acquisition of biologically relevant information contributing to a deeper understanding of biological processes especially used in a synergy with other imaging techniques [18-20].

Common applications reach from investigations on human or animal tissue sections [21-24] over experiments on plant tissues [25] to the analysis of various other biological samples such as synovial fluid [26] or hair samples [27, 28]. Particular attention has been addressed to the investigation of tissue sections with a large number of examined tissue types such as liver, kidney, brain and many more. A special application is the examination of the distributions of metals originating from drugs interacting with tissues. LA-ICP-MS has been utilized to reveal the distributions of platinum in tumour tissue sections being used for tumour treatment in form of inorganic platinum complexes [29, 30]. However, in most reported experiments only quantitative information about the analyte distributions was obtained despite the fact that ICP-MS offers the possibility of providing quantitative results. Even for qualitative measurements the use of internal standards is imperative to compensate for several factors possibly influencing the absolute signal during measurement. The main purposes of an internal standard are the correction of:

- Differing ablation behaviour of the laser due to slight variations in the beam focus or effects of differing matrix composition
- Changing plasma conditions caused by the introduction of different matrices into the plasma or other changes in the experimental conditions
- Variations in absolute signal intensities during measurement time (e.g. instrumental drifts)

Additionally, an optimal internal standard should give the possibility for the compensation of day-to-day variations in the measurement conditions to make data obtained in different experiments comparable [31].

In many experiments the selection of internal standards has only been given minor attention. The number of considered elements possibly acting as internal standards has been mostly reduced to elements naturally occurring in the measured samples. The most prominent example is carbon appearing in every biological sample. However, carbon has been shown to be only appropriate as internal standard under certain conditions and is often unsuitable for reliable quantitative information [32]. The high first ionization potential (11.2603 eV) compared to metallic analytes and the often inhomogeneous distribution on most samples are only two reasons excluding carbon from the list of favourable internal standards.

Internal standards that are not sample-inherent have been of limited interest in the past. Recently proposed concepts are the coating of the sample surface with metallic films [33] or organic polymers doped with trace metals [31] acting as internal standard. The use of gold layers as internal standard has been proposed and tested by Konz *et al*. [33] showing first satisfactory results. Gold layers can be homogenously applied with little experimental effort on a large variety of sample surfaces using sputtering techniques. The simplicity of the application of gold thin-films is an important factor as due to minimal sample handling the risk of contaminations is reduced. Furthermore the ionization behaviour of gold is similar to other trace metals commonly appearing in biological samples as its first ionization potential (9.2255 eV) is comparable with those of elements such as copper (7.7264 eV) or zinc (9.3942 eV).

In the work of Konz *et al.* [33] the quality of the obtained images could be drastically improved by reduction of possible instrumental drifts. However, this approach only delivered improved qualitative information about the analyte distributions.

With the mentioned limitations for qualitative measurements one of the most challenging aspects in LA-ICP-MS imaging is the capability of providing reliable quantitative information. Normally for quantitative laser ablation experiments matrix matched standards are used where homogenized tissues are spiked with the analytes of interest [21]. However, due to high variability and complexity of biological materials those standards are scarcely available and are often not capable of eliminating all sources of possible signal changes. Therefore more sophisticated concepts combining internal standardization methods and easily available standards have to be developed.

During this work the use of gold as internal standard has been tested and evaluated for the use in quantitative imaging experiments. For method evaluation printed patterns on different organic matrices were used considered being a suitable alternative for tissue sections or other biological samples. By proving that also matrix effects can be minimized using gold standardization an accurate quantification approach for imaging experiments could be proposed. After completed method evaluation the obtained experimental conditions were transferred to real samples with unknown analyte concentrations with the aim of spatially resolved quantitative information about the elemental distributions.

2. Theoretical aspects

2.1 Inductively coupled plasma mass spectrometry (ICP-MS)

Inductively coupled plasma mass spectrometry (ICP-MS) is a widely used method within the field of inorganic trace- and ultra-analysis. Several factors make ICP-MS a feasible method for a large variety of applications.

The most important aspects to be mentioned are the high sensitivity and the high dynamic range of the described method. Depending on the analyzed element it is possible to detect analyte concentrations in solute samples in the low ppt scale (pg/L). The linear range of the ICP-MS method is up to twelve orders of magnitude which is also a great pro to be mentioned. Additionally, using ICP-MS it is possible to perform isotope analyses not being accessible to non-mass spectrometric techniques.

2.1.1 Sample introduction

When ICP-MS is used for routine analyses the sample is in most of the cases introduced into the device as a liquid. A wet aerosol is created from the sample using a nebulizer. Other sample introduction techniques commonly used are electrothermal vaporization (ETV) and laser ablation (LA, will be described later) being examples for the direct introduction of solid samples.

2.1.2 Inductively coupled plasma

When the sample aerosol, whether being a wet aerosol from a nebulized liquid sample or a dry aerosol from solid sampling, enters the ICP-MS device it is directly introduced into the inductively coupled plasma.

The plasma jet is formed using a so-called plasma torch made of quartz glass. Figure 1 shows a schematic drawing of a plasma torch mainly consisting of three concentric glass tubes. Through the inner tube the sample aerosol together with a carrier gas is introduced into the center of the plasma jet. The two outer rings serve for the provision of plasma gas (middle tube) and cool gas (outer tube). Typically argon is used for gas supply. Gas flows are around 1 L/min for the nebulizer gas transporting the aerosol and for the plasma gas; commonly used cool gas flows are approx. 15 L/min.

The plasma torch is surrounded by an HF coil serving as the supply of an electromagnetic field for plasma ignition and maintenance of the plasma. For igniting the plasma a high voltage spark is used to ionize the first argon atoms. The formed

atoms interact with the high frequency (HF) electric field generated by a time-varying electric current in the HF coil. More and more atoms get ionized and finally form the plasma which is stabilized by the electromagnetic field from the HF coil. Typical temperatures of the plasma vary between 6 000 K and 10 000 K depending on the HF energy and the applied gas flows.

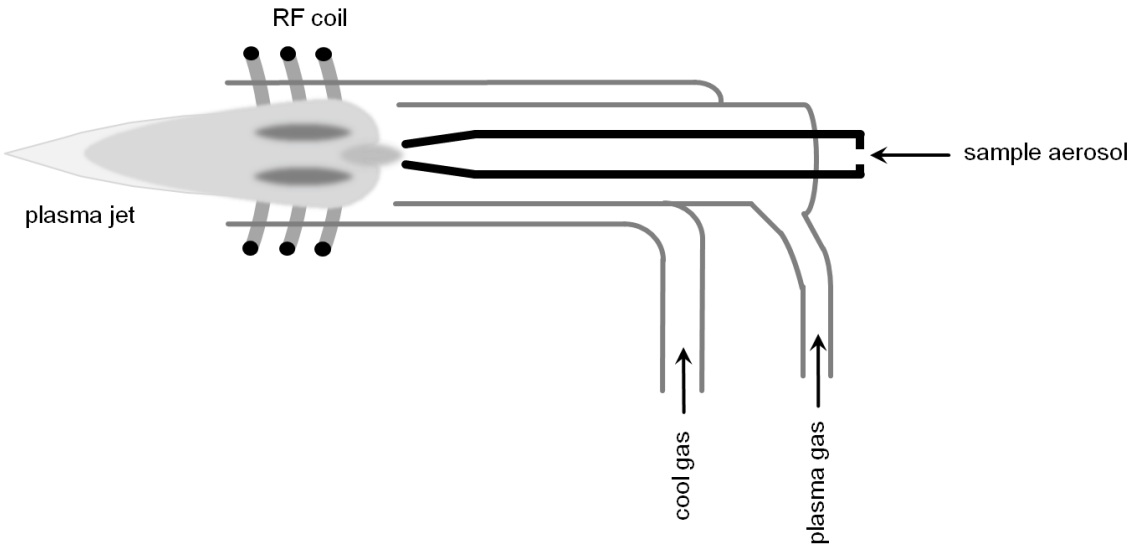

Figure 1: Schematic overview of a plasma torch used for ICP-MS

At the high temperatures in the plasma all analytes are vaporized, present molecules dissociate and the analytes get ionized. The ionization efficiency depends on the first ionization potential (FIP) of the elements; the higher the FIP the less is the percentage of ionized atoms.

Due to the high temperature of the plasma the molecules dissociate and the analytes are ionized. However, also polyatomic ions can form in the plasma being not existent at ambient conditions. Most prominently formed species are ions consisting of the analyte ion and oxygen or argon, elements which are present in high abundance in the plasma. The formed polyatomic species can have similar masses to other analytes (isobaric interferences) and in some cases cannot be resolved using the mass resolutions employed in the ICP-MS devices, especially in quadrupole instrumentations offering only lower mass resolutions. These formed molecules are called spectral interferences.

2.1.3 Vacuum interface

Analyte ionization is performed at atmospheric pressure but separation and detection of the produced ions has to be conducted under vacuum conditions preferably in the range of 10^{-7} to 10^{-8} mbar to increase transmission by decreasing the number of analyte ions that collide with remaining gas molecules. The interface from atmospheric pressure to high vacuum is one of the most challenging aspects of ICP-MS instrumentations.

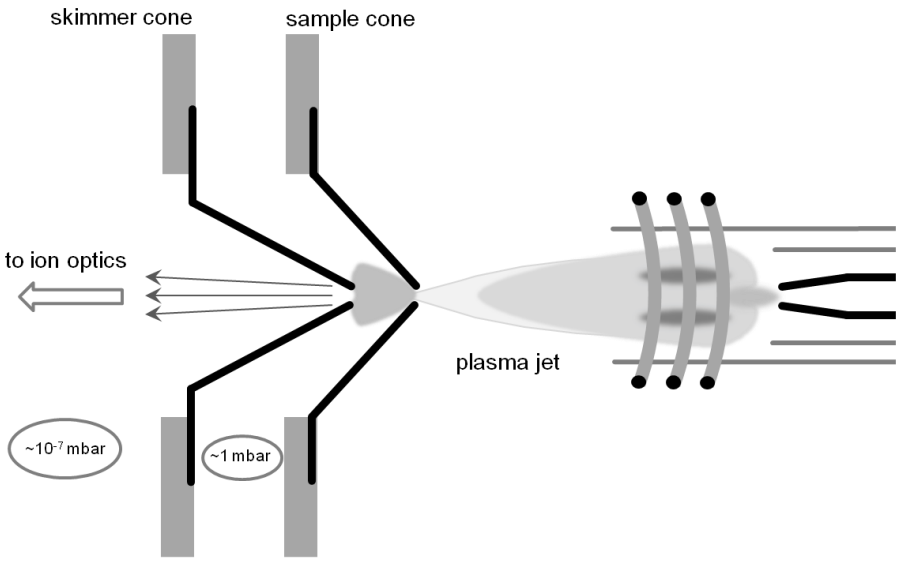

Figure 2: Typical vacuum interface used in ICP-MS devices employing a two step system

This transition is realized using a two step system employing metal parts (cones) with round holes of a diameter less than 1 mm. The interface is schematically shown in Figure 2. These cones are in most of the instruments made of nickel; also platinum cones are available for special applications. The first cone (sample cone) accomplishes the transition into the first vacuum area with a pressure of approx. 1 mbar. From there the second step into the high-vacuum is aided by the skimmer cone with a significantly smaller hole than the sampler come.

2.1.4 Ion optics

The most important role of the ion optics is to focus the ions after transition into the high vacuum to avoid fractionation effects due to different masses of the ions.

The ion optics has a second important use. After the sample flow has been introduced into the high-vacuum it still does not only consist of ions. Neutral atoms that have not been ionized and photons are the most important components to be mentioned. Especially the large number of photons is a major problem when it comes to detection.

Detection capability will be lowered by photons and neutral particles reaching the detector. To overcome this problem the ion optics is used. The ion stream is either deflected off-axis but kept parallel to the plasma torch or is deviated in an angle of 90° depending on the used instrumentation.

2.1.5 Ion separation and detection

Three main concepts of mass analyzers are used in commercially available ICP-MS devices: the sectorfield, quadrupole and time-of-flight (ToF); sectorfield and ToF will not be described here in more detail as only a quadrupole device has been used during the presented experiments. Only one point should be mentioned here: Sectorfield devices offer higher mass resolutions than quadrupoles serving as high resolution MS devices. ToF devices allow for simultaneous detection of the whole mass spectrum which is not possible with the other types of mass analyzers. In comparison to the sectorfield the obtainable mass resolution of quadrupole instrumentations is significantly lower, however scan speed is high compared to sectorfield devices allowing for highly time resolved measurements with the detection of multiple analytes in a quasi-parallel way (close to simultaneous detection in ToF devices). Figure 3 shows a schematic drawing of a quadrupole mass analyzer.

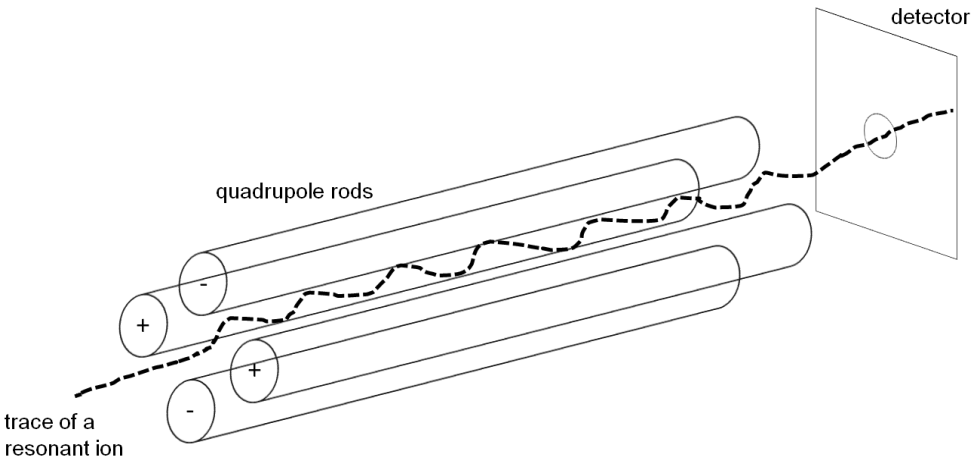

Figure 3: Quadrupole mass analyzer used in ICP-MS devices

The quadrupole mass analyzer separates ions by their mass-over-charge (m/z) ratio. As the name implies the quadrupole consists of four cylindrical metal rods on which differing voltages can be applied. One quadrupole setting allows only ions with a specific m/z ratio to pass the quadrupole. This ion passes the quadrupole at a resonance frequency; all other ions are deflected. By changing the voltages the m/z ratios to be analyzed can be varied within a short time scale. Before the ions are separated in the

mass analyzer a collision cell can help to reduce the number of molecular species. The introduced collision gas (He, H_2) will collide preferably with species with great size i.e. the polyatomic ions. The method of the collision cell will not be explained in further detail here as it has not been used in the experiments for this work.

The separated ions proceed to the detector which is in the majority of the cases an electron multiplier. An ion hitting the dynode will cause the emission of a secondary electron. This electron is the starting point of a chain reaction causing a multiplication of the signal.

2.1.6 Quantification

In contrast to other mass spectrometric methods ICP-MS can be easily used for absolute analyte quantification in liquid samples. Therefore external calibration is used employing standard solutions with known analyte concentrations. Additionally internal standards are often used in ICP-MS experiments to compensate for matrix effects and instrumental drifts. The use of internal standards will be described later in more detail.

For solid sampling experiments the task of quantification is by far harder to achieve. Here standards being similar to the sample material are required to avoid matrix dependent ablation changes and various other aspects. Due to the large variety of analyzed samples these standards are often not commercially available and have to be prepared in-house.

2.2 Laser ablation (LA) and coupling with ICP-MS

With the invention of the laser in 1960 [34] soon strategies for the coupling of laser ablation and mass spectrometry (LA-MS) have been developed. However, more than 20 years have passed to discover a method capable of multi-elemental analysis in combination with laser ablation. The developed methods were LA-ICP-AES [35] and LA-ICP-MS [36] thereof the latter allowing not only for direct multi-elemental analysis but also for isotope analyses.

For ablating sample material the sample is placed in an air tight sample chamber which is flushed by an inert gas (in most of the cases helium) before material ablation. The sample is attached to a mechanical stage allowing for translations in x, y and z direction allowing for spatially defined material ablation. When the laser fires on the sample material is ablated and an aerosol is formed which is then transferred to the analyzing device using a carrier gas (in most routine applications helium). The laser spot diameter

is variable and can be chosen according to the analyzed sample type and the desired spatial resolution of the analysis. After reaching the plasma source of the coupled device the processes are comparable with those described earlier. A schematic overview of an LA-ICP-MS device is presented in Figure 4.

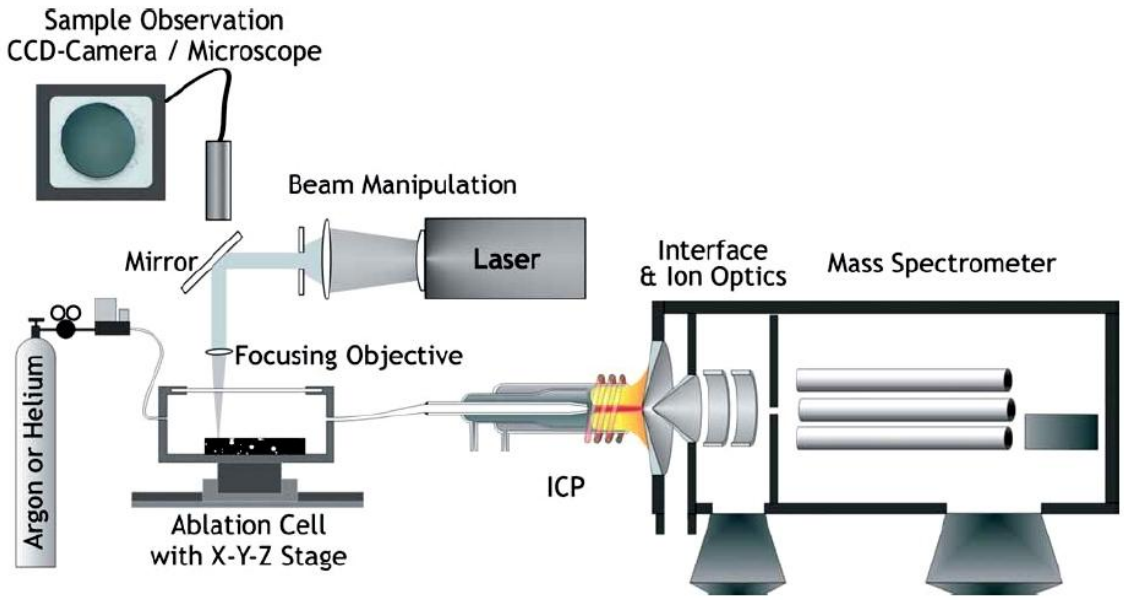

Figure 4: Schematic overview of a laser ablation (LA) system coupled to an ICP-MS instrumentation [8]

The simplicity of laser ablation has attracted a lot of attention. Especially the simplicity of the method allowing for fast analyses and the high sensitivity when coupled with ICP instrumentations have to be mentioned.

Within the last decades the properties of used lasers have rapidly developed and many improvements have been made. Two important specifications of the laser have to be pointed out here. The first is the laser wavelength. The lower the wavelength the more the material ablation is independent from material properties such as color and absorption differences and with lower wavelengths also the applied energy density on the sample will be increased. With the first lasers working in the IR or visible wavelength range it was only possible to ablate a limited selection of materials and the ablation efficiency strongly depended on the color of the sample. With the development during time lasers with wavelengths in the low UV range have been produced. Nowadays typical lasers used for LA have wavelengths of 213 nm (solid-state laser, e.g. Nd:YAG) or even 193 nm (gas phase laser, e.g. ArF-excimer) with optimized absorption properties. The second important point is the laser pulse duration. The shorter the pulse duration of the laser the sharper is the created laser crater. Melting

effects of the ablated material should be avoided and fractionation effects may appear with longer pulse durations meaning that not all elements will be ablated from the sample with the same efficiency. This effect will hamper reliable quantification. Most lasers used today use pulse durations in the nanosecond range. Also femtosecond lasers have been developed with superior ablation properties and reduced effect of elemental fractionation. However, the acquisition thereof has a major financial aspect.

As the ablation is not material independent and will be significantly different for example on metallic samples compared with biological materials. Therefore for quantitative determination of the elemental composition of the sample matrix-matched standards have to be employed. For some materials certified reference materials (CRM) with exactly determined trace element concentrations are available. However, due to the large variety of analyzed samples the preparation of matrix-matched standards has to be often done in-house involving a great experimental effort.

Despite the mentioned limitations LA is a widely method especially coupled with ICP-MS instrumentations. Some outstanding features have made LA an often used tool for elemental analysis of various sample types. As described in the following chapters LA-ICP-MS is also a feasible method for the analysis of biological samples.

2.3 ICP-MS for the analysis of biological samples

Even though ICP-MS is often used for the analysis of inorganic samples within environmental chemistry, geology and other fields of science the mentioned technique is also often applied in countless applications on biological samples [7]. The determination of trace metals in biological tissues as signs for intoxication as well as protein quantification are only two applications of the trace elemental analysis in bio-samples. Trace elements in tissues are of special interest and vary within different organs of the investigated organism [37]. However, organisms do not only contain trace metals due to unwanted uptake from the environment from polluted air; the appearance of trace metals is often linked to proteins using metal ions as cofactors (metalloproteins). Properties of this subclass of proteins will be described in one of the following chapters.

Besides the analysis of trace elements directly in tissues ICP-MS is also used for the detection and quantification of extracted and optionally electrophoretically separated proteins in synergy with immunoassays [5]. An antibody being highly specific for the

protein of interest will bind to the protein and a chelate complex containing an rare earth element will bind to the antibody. Then the amount of bound rare earth element can be determined using ICP-MS with high sensitivity. It is also possible to use the antibody linked metal-tagging with laser ablation [3].

2.4 Imaging experiments using LA-ICP-MS

Revealing the spatial distribution of analytes in various kinds of samples can provide fundamental information about the sample properties and can help to improve the understanding of different processes. Not only but especially in biological samples (e.g. tissue samples) the depiction of analyte distributions can be of special interest. The process to visualize those analyte distributions is called imaging. In the field of medical sciences the expression imaging describes a far larger field for techniques being used not only to depict the distributions of single analytes. Imaging in medicine is an overall term for the visual representation of processes within an organism. Prominent examples to be named are magnetic resonance imaging (MRI) or positron emission tomography (PET) both being examples for nuclear medical imaging. First publications in the field of life sciences dealing with various types of imaging date back to the 1950s-1960s.

However, the technique used during the present work does deal with mass spectrometric imaging, especially laser ablation imaging. Due to the principals of LA-ICP-MS described earlier it is possible to depict elemental distributions on the sample surface. The material is ablated and completely dissociated in the inductively coupled plasma leading to the possibility of elemental analyses of the sample being almost independent from the sample material. Some limitations will be described later.

Laser ablation imaging on biological samples is mostly performed on tissue samples [21, 22, 38, 39] but also on other biological materials such as hair samples [27, 28].

For the imaging of tissues the sample material has to be first cut into thin sections using a microtome as a complete tissue sample cannot be directly placed in the ablation chamber. Typical thicknesses of the cut tissues are between 1 and 10 µm; ultra-thin sections can be only a few hundred nanometers thick being used for special cases. Before cutting the sample may undergo several stages of pretreatment. Most common technique in histopathology is that the tissues are fixed with formalin (an aqueous solution of formaldehyde, effects cross-linkage of the proteins) and the material is embedded in paraffin [40]. During this procedure soluble components are removed or

may be distributed over the whole sample due to diffusion. After being embedded in paraffin the samples are cut using a microtome. The paraffin can be removed from the cut sections.

Other procedures for cutting do not involve such a long process for sample pretreatment. Also raw tissues can be used for cutting maintaining the position of all analytes within the tissue. The main reason that mostly paraffin embedded tissues are available for analyses is that this technique is a common practice in the medical sciences and other samples are scarcely obtainable. Paraffin embedded tissue samples can be stored at room temperature for several decades whereas other samples need special storage conditions.

After cutting the tissue sections are attached onto glass slides for further analysis. The glass slide can be easily placed in ablation cells of common size. To allow for at least meaningful or at the best quantitative analyses the sample material should be completely ablated which is normally no problem at tissue sections with a maximum thickness of 20 µm.

In principle two analysis modes for the acquisition of image data are available for LA-ICP-MS experiments. As the ICP-MS device can record time resolved intensity data for all chosen elements either spot scan or line scan can be employed. Schematic drawings of the two scan types are shown in Figure 5.

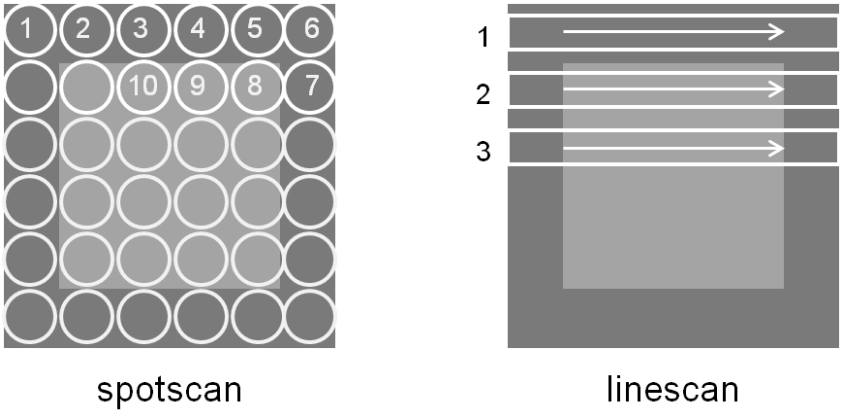

Figure 5: Scan types available for LA-ICP-MS imaging experiments; linescan can also be employed with alternating scan directions in every line

For the spot scan the laser is fired for a defined time onto one single point of the sample. Then the laser firing is stopped to allow the ablated material to be washed out from the ablation cell. After this pause the next spot is ablated. As after every spot a pause has to

be made this imaging technique is not very time efficient. Therefore the linescan is preferred in most experiments. Here the laser is fired on the sample surface and moved in one direction over the sample with a defined scan speed. After the first line has been ablated the laser moves to the next line. With the known scan speed the position of the laser can be calculated for every time point. Compared to the spot scan pauses can be avoided given that the wash-out time of the ablation chamber is small enough to prevent the resulting images from being blurred in the scan direction.

During method development the laser parameters such as repetition rate (typically up to 20 Hz), laser beam diameter, scan speed and laser energy have to be optimized. The most crucial parameters are laser beam size and scan speed. The beam diameter determines the obtainable spatial resolution of the resulting distribution images. The smaller the beam diameter the better is the resolution. However, with decreasing beam diameter less material will be ablated and less amount of analyte can be detected. With a halved beam diameter only a fourth of the material will be ablated. Especially when coming to ultra-trace analyses this is a not negligible aspect. A second important point concerning the laser spot size is the time of the measurement. As the whole sample has to be rastered laser spot size and scan speed determine the measurement time. The scan speed can be chosen arbitrarily but has an applicable maximum depending on the laser diameter. So the time of the measurement is firstly determined by the spot size. A short example will be given later to illustrate this fact. Typically applied laser diameters for imaging experiments on biological samples are between 10 and 100 µm depending on the sample to be analyzed and the desired spatial resolution.

Optimizations of the scan speed have been made earlier in literature [41]. The results show that even scan speeds with the values of the laser diameters multiplied by five may be applicable. However, typical scan speeds are equal to the value of the laser diameter (e.g. 50 µm laser spot size – 50 µm/s scan speed) to avoid a distortion of the resulting image. Scan speeds being smaller than the laser diameter have shown to yield not improvement in image quality but only extend the acquisition times.

An example should illustrate effect of the choice of the laser diameter on the time used for acquisition. The scan speed is set to a value being even to the laser diameter for this example. At a laser diameter of 50 µm the acquisition time for a sample of 1 x 1 cm in size is approx. 11 h. With the laser diameter decreased to half of the value (25 µm) the acquisition time multiplies by four to more than 44 h as also the scan speed has to be

halved. This means a considerable difference to the 11 h for only doubling the spatial resolution of the resulting images.

2.5 Problems in qualitative and quantitative imaging experiments

The differing ablation properties of changing materials have been described earlier. The same limitations also apply for imaging experiments on biological samples. Using LA-ICP-MS it is possible to quantify the amount of analyte in the sample; however, in most of the cases matrix-matched standards are used to compensate matrix dependent ablation differences. These standards are prepared by homogenization of tissue material and spiking the homogenate with different amounts of trace elements to be analyzed. The material is pressed and thin cuts are made to yield standards comparable to the samples but with known analyte concentrations. By the preparation of matrix-matched standards an ‘average’ of the sample material is created. Different sample conditions within one tissue slice are not taken into consideration neglecting the ablation differences being possible on different areas of the tissue. For example areas higher in the concentration of lipid compounds may show alternated ablation behavior to other regions on the sample. Despite the same amount of analyte the absolute signal reaching the detector possibly varies.

The second important aspect in LA-ICP-MS measurements is the instrumental drift. As described before acquisition times for elemental images are rather long. During this time a large amount of material is ablated which can partly be deposited on the cones or on lenses leading to an alternated response of the instrument. Furthermore the vacuum conditions may change slightly during measurement time or the gas flows can vary within a small range possibly leading to changed plasma temperature. Thus within one experiment the instrument sensitivity may change resulting in different signals for sample areas with equal analyte concentrations.

The standards are measured followed by the measurement of the sample itself. Possible signal changes due to the described aspects are not taken into consideration.

To overcome the mentioned limitations internal standards have to be employed compensating for all appearing changes of the absolute signal intensity. The choice of appropriate internal standards is a challenging task and many aspects have to be taken into consideration. Principally two types of internal standards can be used. Analytes appearing in the sample as well in the standard material with homogenous distribution

may be used for signal normalization. A prominent example thereof is carbon. However, often not being distributed evenly on the sample it is often used as internal standard. Several other aspects like the high first ionization potential (11.2603 eV) compared to other analytes (around 7-9 eV for common metals) and the high background signal would normally eliminate carbon as a suitable internal standard. In the past a 'better-than-nothing strategy' was dominant and the use of carbon was considered being better than using no internal standard at all even taking the risk of introducing artefacts.

In the near past new concepts for internal standardization have been developed though not being applied in a wide range of studies. The novel standardization strategies involve additionally applied internal standards like rare trace metals in polymeric films [31] or gold thin-layers applied by sputtering [33]. Advantages thereof are complete homogeneity of the distribution over the sample surface and independence from sample conditions.

2.6 Metals in biological tissues

Metals may appear in biological tissues in different forms: either solute in their free form, in complex compounds with small molecules or bound to specific proteins (metalloproteins). 99% of the mass of a human organism is formed by only 11 elements (N, C, Ca, Na, Cl, K, H, P, O, S, and Mg) [42] thereof being only four metals. So, all other metals in tissues will be trace elements appearing only in minor concentrations. 47% of all proteins listed in The Protein Data Bank (PDB) [43] contain at least one metal ion. Another important aspect is the uptake of metals from the environment being not essential for biological processes and possibly acting as toxins.

2.6.1 Metals appearing in ionic form

Metals appearing in ionic form are mostly metals of the first and second group of the periodic table of elements acting as electrolytes (especially Ca, K, Na and Mg). Concentration differences and gradients are essential for the maintenance of the stability of cell walls and intracellular structures [44]. Another important aspect of alkali and earth alkali metals is signal transport [45]. Proteins fixed in the cell walls (ion channels) are capable of selectively transporting ions and therefore can form a concentration gradient. One prominent example are Na/K-ATPases being able to form a Na/K gradient driven by the degradation of ATP. Metal transport phenomena are also involved in signal forwarding by nerves and in muscle contraction.

2.6.2 Metals as cofactors in proteins

Transition metals are abundant in organisms only in trace concentrations. These elements do not appear in organisms in free form but are bound to specific proteins utilizing them as cofactors to obtain their catalytic activity. The metal ions can be directly bound to the protein structure or use a small organic complex to maintain the binding to the protein.

Most abundant trace metals in biological tissues of animals are iron and zinc [46]. Important proteins utilizing metallic cofactors are catalase, hemoglobin or metalloproteinases.

Some other common metalloproteins act as hydrolases (carbonic anhydrase, metallophosphatases and metalloproteinases). Hydrolases catalyze the cleavage of a chemical bond; the involved metals are used as reducing or oxidizing agent being directly involved in the reaction.

Other often appearing metalloproteins are electron-transfer proteins (cytochromes, iron-sulphur proteins and copper proteins) [47]. These electron-transfer proteins are complementary to the non-metallic electron transporters nicotinamide adenine dinucleotide (NAD) and flavin adenine dinucleotide (FAD).

Further metalloproteins are responsible for processing small gaseous molecules such as oxygen (myoglobin, hemoglobin) or carbon dioxide [48]. In oxygen processing proteins the organic iron complex Heme is utilized as metal core binding the molecular oxygen.

A special case for metals in biological complexes is vitamin B12. It is an organic complex with cobalt as core atom. Vitamin B12 is used as a cofactor by various proteins for example by methionine synthase. Also molybdenum seeming a rather scarce element in biological systems is used as cofactor in various proteins [49].

This list of examples for metals in biological tissues shows the large variety of use for metallic species in biochemical processes.

2.6.3 Toxic metals

Some metals have no biological use and form poisonous soluble compounds. Important metals that have to be mentioned are cadmium, lead, mercury or radioactive metals such as uranium or plutonium. Also biologically important trace metals like iron, nickel or

chromium can act as toxic compounds when occurring in higher concentrations or in specific oxidation states.

Especially heavy metals can accumulate in tissues as they cannot be degraded in the same way as organic toxins. This is one of the main reasons for the high severity of toxic metals. The interactions with biological material are various. Many metals interact with DNA during replication and therefore are carcinogenic and mutagenic [34]. Other effects of metal poisoning can be allergies (reaction to nickel), neurological diseases (mercury) and other diseases.

2.6.4 Metals in medical applications

Chemical compounds containing metals are often used for diagnosis or disease treatment. Technetium or gadolinium are employed for imaging purposes in magnetic resonance imaging. Complex compounds containing these elements act as a contrast agent during diagnostic examinations.

Some noble metals are used for the treatment of diseases. Platinum has to be named here being a prominent example for metals used in pharmaceuticals [50]. Organic complexes containing platinum as core atom inhibit cancer growth and are in many cases used for cancer treatment.

3. Experimental

3.1 Instrumental

During this work quadrupole ICP-MS instrumentation (Thermo iCAP Q, ThermoFisher Scientific, Bremen, Germany) was used. The system separates ions from photons and neutral atoms employing a 90° deflection lens. This improves the sensitivity especially for low mass ions. Data acquisition was performed using Qtegra software provided with the instrument.

An image of the used device is shown in Figure 6.

Figure 6: ThermoFisher Scientific iCAP Q ICP-MS instrumentation used for the performed experiments

Solution nebulization ICP-MS measurements of digested samples were carried out using a peltier cooled spray chamber equipped with a concentric quartz glass nebulizer for sample introduction; samples were introduced employing an ESI SC-2DXS autosampler (Elemental Scientific, Inc., Omaha, NE). Instrument parameters were optimized on a daily basis for maximum ^{115}In and signal and minimum $^{140}Ce^{16}O/^{140}Ce$ ratio using a tuning solution provided with the instrument. Measurements were carried out employing the standard measurement parameters recommended by the manufacturer.

For solid sampling a commercially available laser ablation system (New Wave 213, ESI, Fremont, CA) equipped with a frequency quintupled 213 nm Nd:YAG laser was employed. The used ablation cell allows the measurement of larger samples as in

conventional laser ablation devices. With the use of an ablation cup which is always kept directly above the currently ablated sample area a rapid washout behavior is ensured.

Using tubing between LA and ICP-MS the connection of the two devices was established. He carrier gas was employed to transport the ablated sample material from the sample into the plasma. During all measurements dry plasma conditions were applied.

The used laser ablation device is presented in Figure 7.

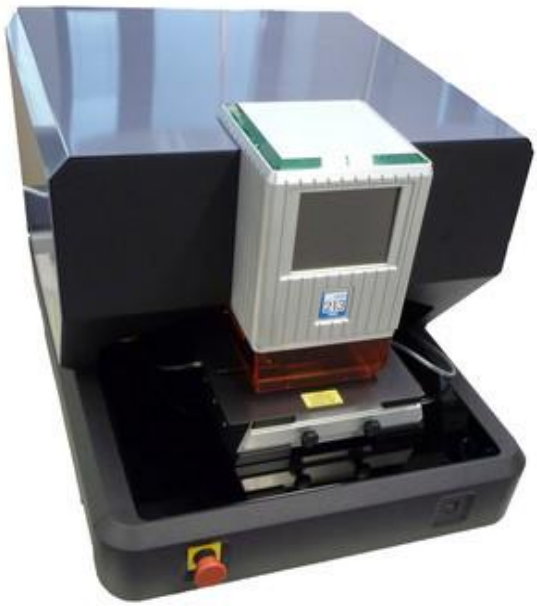

Figure 7: New Wave 213 laser ablation device employed for the performed experiments

Laser energies were optimized to reach complete ablation of the material but still providing controlled ablation conditions; the laser beam diameter was adjusted to a value being the best compromise between obtained resolution and amount of ablated material.

The measurement parameters concerning the MS instrumentation were optimized using NIST 612 trace metals in glass standard (National Institute of Standards and Technologies, Gaithersburg, MD) for maximum ^{115}In signal before every experiment; typical parameters used for the sample measurements are shown in Table 1.

laser ablation system	***New Wave 213***
average fluence	4.9 J/cm²
laser diameter	50 µm
scan speed	50 µm s^{-1}
repetition rate	10 Hz
carrier gas flow (He)	1 L min^{-1}
ICP-MS instrumentation	***Thermo iCAP Q***
aux. gas flow	0.8 L min^{-1}
cool gas flow	15 L min^{-1}
dwell time per isotope	0.01 s
RF power	1550 W
cones	Ni
measured isotopes	^{13}C, ^{63}Cu, ^{65}Cu, ^{197}Au

Table 1: Typical parameters of the laser ablation and ICP-MS instumentation

For the imaging experiments a focused laser beam with 50 µm beam diameter and a scan speed of 50 µm s^{-1} was utilized for all documented imaging experiments. Data for the images were acquired after creating line scan patterns; single lines were drawn in the laser control software and then duplicated multiply to create a rectangular line scan pattern over the sample surface. Before starting the measurement the laser was allowed to warm up for 20 s by firing on a closed shutter. During measurement laser firing was stopped at the end of each line, the crosshairs moved back to the left edge of the sample and ablation started again in the next row. So, the scan direction of every line led from the left to the right side of the sample. The created interruptions in the recorded signal intensity for ubiquitous analytes (e.g. ^{197}Au) allowed for automatic recognition of the position and number of measured lines for image construction.

Microscopic images were recorded using a Leica DM2500M microscope (Leica Microsystems, Wetzlar, Germany) in reflected light mode.

3.2 Preparation of printed patterns

The patterns printed on high gloss inkjet photo paper (280 g m^{-2}; Office Depot Europe B.V., Venlo, The Netherlands) and inkjet transparency foils (Thalia Buch & Medien GmbH, Linz, Austria) were designed in Microsoft PowerPoint 2007 (Microsoft Corp, Redmond, WA) and printed using an HP Deskjet D4260 inkjet printer equipped with an HP 350 black cartridge and an HP 351 tri-colour cartridge (Hewlett-Packard, Palo Alto, CA). Patterns with multiple 400-µm-squares in different transparency settings (0, 25, 50

and 75%) were designed. The patterns were printed with cyan ink (RGB index 0,255,255) containing an organic copper complex providing the blue color. Print resolution was set to the maximum value of 600 x 600 dpi; different software settings were evaluated to yield optimal printing results in terms of reproducibility and resolution.

3.3 Sample preparation

Printed inkjet patterns were attached to glass slides using double sided tape (3M, St. Paul, MN) for further processing and measurement. To measure both patterns in one imaging experiment a combined sample with transparency foil and photo paper was fixed on a glass slide in a way that the minimal possible gap was between the two printed patterns giving the possibility.

The samples mounted on glass slides were metalized 30 s with gold. The coating process was performed using an Agar B7340 sputter coater (Agar Scientific Limited, Essex, UK) equipped with a gold sputtering target. Distance from sample to the gold target was adjusted to 4 cm before every sputtering process. Time required for metallization were optimized during method development and kept constant for every experiment to obtain comparability of different analyses. The sputtering current was set to 10 mA and before sputtering the sample cell was evacuated to a pressure of approx. 0.1 mbar.

After completed sample preparation and placing the sample in the chamber the ablation chamber and the gas lines were purged with He carrier gas at 0.5 L min^{-1} for 1 h before every measurement.

3.4 Image construction

Time resolved intensities for the measured isotopes recorded with the Qtegra software were exported as *.csv* files. ImageLab (v.0.40, Epina GmbH, Pressbaum, Austria) was used for further file processing. The files were imported and the scanning mode (line or point scan) and the scan direction were selected. The vertical number of pixels was automatically calculated by the number of detected lines whereas the horizontal resolution could be set manually. Elemental images were created and different statistical tools included in the mentioned software package were utilized for ongoing analyses. The software utility also allows for correction to internal standards and the overlay of elemental distribution and visual image for optical correlation of visible structures with

the elemental distributions. All constructed images had a spatial resolution of 50 μm in both horizontal and vertical direction.

4. Results and discussion

Samples being available in a high number of comparable replicates are favorably used for reliable method development as variations in the results are then only depending on the employed method and cannot be traced back to sample variations. As biological tissues cannot be reproducibly produced and no tissue section will be like the other an alternative material for method development had to be utilized. Photo paper and transparency foil were chosen being comparable to tissue sections by carbon content, density and other parameters. In contrast to tissue sections the mentioned matrices can be printed using an inkjet device producing reproducible samples in terms of analyte concentrations. A further advantage of the inkjet patterns is that the analyte concentration can easily be determined by solution nebulization ICP-MS confirming that all printed patterns are comparable.

4.1 Copper concentrations on the printed samples

The thesis that normalization to an internal standard should yield equal intensity values for material ablated from different matrices is only valid if the deposited amount of copper is equal on the investigated materials. Thus before carrying out laser ablation experiments the comparability of ink deposition on the materials used for printing had to be shown. Solution nebulization ICP-MS seemed to be the most straightforward method for the determination of analyte concentrations after conversion of the prepared samples into liquids.

For exact determination of the copper concentrations on photo paper and transparency foil the printed squares with different transparency levels were cut out and completely mineralized using 400 µL conc. HNO_3 (p.a., Merck, Darmstadt, Germany) and 100 µL 30% H_2O_2 (p.a., Merck, Darmstadt, Germany). The amount of copper for every transparency level was determined in triplicates. The reaction was carried out in 10 mL PE tubes at room temperature. After a reaction time of 2 h the mixture was diluted to an overall volume of 5 mL with high purity water (resistivity 18.2 MΩ cm) dispensed from a Barnstead EASYPURE II water system (ThermoFisher Scientific, Marietta, OH) resulting in clear solutions. Indium standard (indium standard for ICP, Sigma-Aldrich, Buchs, Switzerland) was added to a final concentration of 1 µg L^{-1} serving as internal standard. Aqueous calibration standards with copper concentrations in the range of 0.5 to 5 µg L^{-1} (ICP multi-element standard solution VIII, Merck, Darmstadt, Germany) were used for signal quantification.

Derived concentrations varied between 0.05 ppb copper in the blank and 0.2 to 2 ppb copper in samples with different amounts of printed ink. With the low amount of copper in the blank solutions the fact that all measured copper derives from printed ink could be underlined.

Standard deviation of the obtained copper concentrations is very low (overall less than 3%) indicating reproducible deposition of ink on the same matrix. Furthermore it could be shown that the amount of deposited copper on photo paper and on transparency foils does not differ significantly as the determined copper amounts on transparency foil and photo paper vary within the standard deviation of the replicates. Overall it can be stated that ink deposition is equal on replicates of the same matrix as well as on different matrices. The determined amounts of copper are listed in Table 2. By the known size of the printed squares the amount of copper per square millimeter could be calculated [ng mm^{-2}].

Table 2: Copper concentrations on printed squares on photo paper and transparency foil determined using solution nebulization ICP-MS

transparency setting [%]	*copper concentration on foil [ng mm^{-2}]*	*copper concentration on paper [ng mm^{-2}]*
0	5.35 ± 0.10	5.45 ± 0.10
25	2.62 ± 0.03	2.64 ± 0.02
50	0.99 ± 0.03	1.01 ± 0.03
75	0.34 ± 0.02	0.35 ± 0.03

4.2 Distribution of gold on the sample surface

For reliable use of an internal standard the deposited gold layer has to be homogeneously distributed over the sample surface. Thus before the use of gold as internal standard it had to be shown that sputtering creates homogenous metallic layers on a sample surface as well as that gold is deposited equally on different matrices.

For proving that gold deposition is homogenous on the same matrix a glass slide was coated with gold under the routinely used conditions. Sixteen sample areas distributed on an overall area of 2.5 x 2.5 cm were selected and using spot ablation mode (repetition rate 10 Hz, beam diameter 50 µm, dwell time per spot 5 s) the intensities of ^{197}Au were recorded. For every selected area eight spots within 200 x 200 µm were ablated to allow for statistical analyses. The means of each spot were compared using

one-way ANOVA in the statistical software package DataLab (v.3.511, Epina, Pressbaum, Austria).The sixteen resulting means calculated from eight values each were compared using one-way ANOVA. The statistical analysis did not indicate that the means differ significantly ($\alpha = 0.99$; data not shown). Overall RSD of the signals was below 5% ($n = 16$).

To make sure that gold deposition is independent from differing matrices gold was sputtered on photo paper and transparency foil. The determination was performed in triplicates for every matrix. Pieces of equal areas were cut out and digested with 400 µL aqua regia. After allowing 1 h for reaction the mixture was diluted to an overall volume of 9 mL with 1% HNO_3 and the gold content was determined using solution nebulization ICP-MS. Results show that the gold deposition does not vary on different matrices. The concentrations of gold in the sample solutions were 259.1±8.5 ng/L for photo paper and 266.0±8.4 ng/L for transparency foil, respectively.

The obtained results indicate that gold deposition is homogenous on a large area on the same matrix as well as on different matrices making gold layers suitable as internal standard in terms of material deposition.

4.3 Gold as internal standard for the correction of instrumental drifts and matrix dependent ablation differences

Occurring instrumental drifts during time as well as different ablation behavior due to changing matrices should be eliminated by correction of the analyte signals to the ^{197}Au intensity.

The usability of gold as internal standard was tested in imaging experiments with a printed pattern on different matrices. The printed pattern consisted of 24 400-µm-squares printed with cyan ink. The squares were applied in four transparency levels (0, 25, 50 and 75%) in six replicates each. For comparison of different matrices the pattern printed on photo paper, transparency foil was employed.

A schematic drawing of the paper-foil sample is presented in Figure 8.

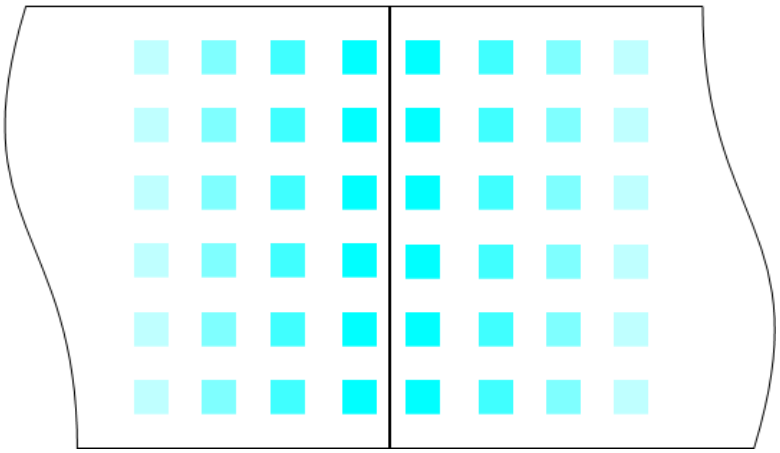

Figure 8: Schematic drawing of the sample with the inkjet pattern used for method development; used matrices were transparency foil (left) and photo paper (right)

During the imaging experiments the isotopes ^{13}C, ^{63}Cu, ^{65}Cu and ^{197}Au were monitored. The samples were scanned using line scan patterns. Employed laser energies yielded a quantitative ablation of the printed inkjet pattern. Complete ablation was proven by a second scanning over the sample where the signal for copper did not exceed the background signal.

Resolution of the obtained images was 130 x 100 points on an area of 6.5 x 5 mm resulting in a spatial resolution of 50 µm in both vertical and horizontal direction. Typical acquisition times of printed pattern samples were approx. 4 h. The distribution of the copper isotope ^{65}Cu is comparable to ^{63}Cu; signals for ^{63}Cu and ^{65}Cu showed linear correlation with a slope (2.2449) being equal to the natural isotope ratio (2.2414) proving that the signals were not influenced by any interference.

Figure 9a represents the distribution of copper (^{65}Cu) on the pattern printed on transparency foil and on photo paper without gold correction. Start of the measurements was in the left upper corner of the images. The four columns of squares on the left side represent the pattern printed on transparency foil where as the right four columns show the print on photo paper. Figure 9b shows the distribution of copper (^{65}Cu) after normalization.

In the uncorrected distribution of ^{65}Cu (Figure 9a) the intensity values for squares in one row clearly represent the changing amounts of ink applied by the printer. Squares corresponding to the highest transparency setting deliver the lowest signal intensity and vice versa as expected by the different amounts of deposited ink. Besides the

concentration difference the size appears to be even for all 24 printed squares underlining the accordance of elemental distribution and printed pattern.

For squares with the same print setting (in one column) a decrease in absolute signal intensity from the first to the last row can be visually declared. After gold standarization (Figure 9b) the described loss in intensity is eliminated and optically no difference between the rows can be identified. This outcome hints to the presence of instrumental drifts during the measurement causing reduced signals with ongoing analysis time.

For numerical demonstration of the effects of normalization the mean intensities of each square were used. An average of the central pixels of each square was calculated, pixels on the edge of the squares were excluded from averaging. Discussion and interpretation of the derived results is presented in the following part.

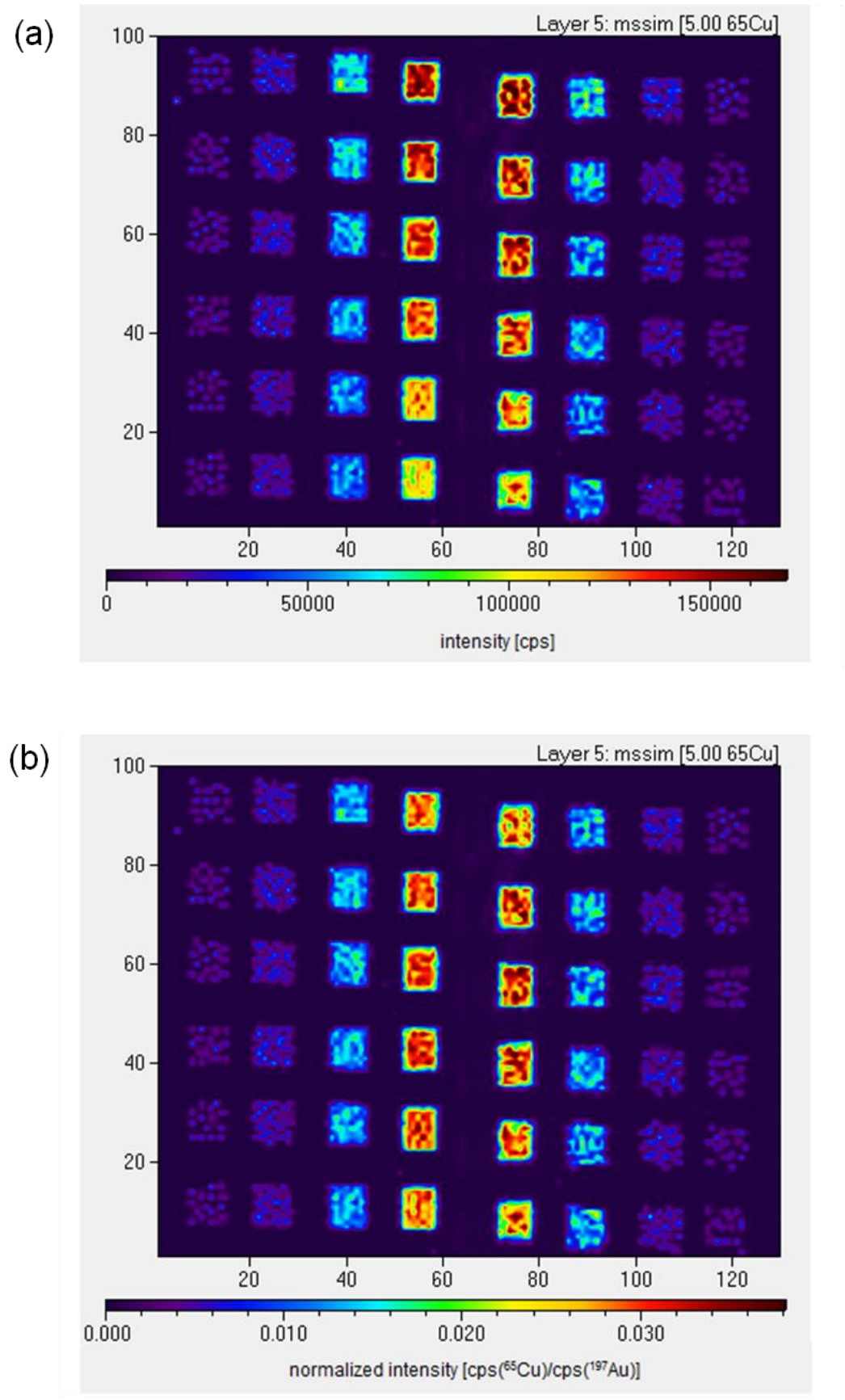

Figure 9: Distribution images of ^{65}Cu on patterns printed on transparency foil (left side of each image) and photo paper (right side of each image) without (a) and with (b) gold correction

4.3.1 Correction of instrumental drifts

The different transparency levels are respresented by different amounts of applied ink. Therefore the set transparency level can be correlated with the actual amount of copper on the samples. Considering the determined copper concentrations by solution nebulization ICP-MS regression lines consisting of four concentrations each for every matrix and every row could be calculated resulting in twelve linear regressions for the presented distribution image. Correlation coefficients of all regressions were above 0.99. Figure 11a shows a straight-line regression of the first and the last row of squares printed in different transparency levels on photo paper. Only row one and six are shown here, the other regression lines lie in between these two showing constantly decreasing slopes. The two shown regression lines differ significantly whereby the absolute value of the slope of the last line is only 75% of the first one. The fact that the slopes of the two regression lines are not even can be ascribed to instrumental drifts resulting in an overall loss of instrumental sensitivity over measurement time.

The appearance of the instrumental drift is comfirmed by the analysis of the ^{197}Au signal. It shows a constant decrease during the measurement time presented in Figure 10. The gold signal decreases more than 20% from the first to the last measured line.

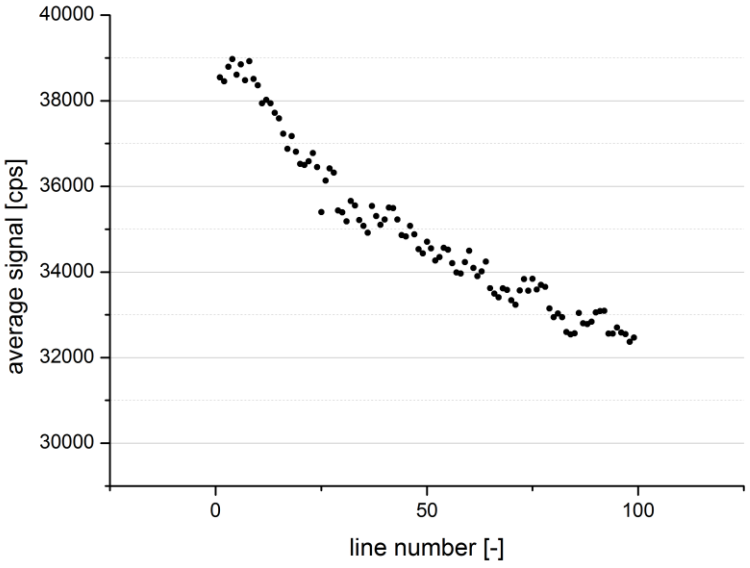

Figure 10: Average gold signal in one line during measurement time

Normalization to the gold signal eliminated the mentioned difference (Figure 11c) as all analyte signals are affected by this drift. After standardization all regression lines have

slopes with comparable values with an RSD of less than 3%. The same observations were made for patterns printed on transparency foil (Figure 11b and d). The result that the internal drift correction is not only valid on photo paper but also on another matrix underlines the applicability of the gold standardization method for instrumental drift correction.

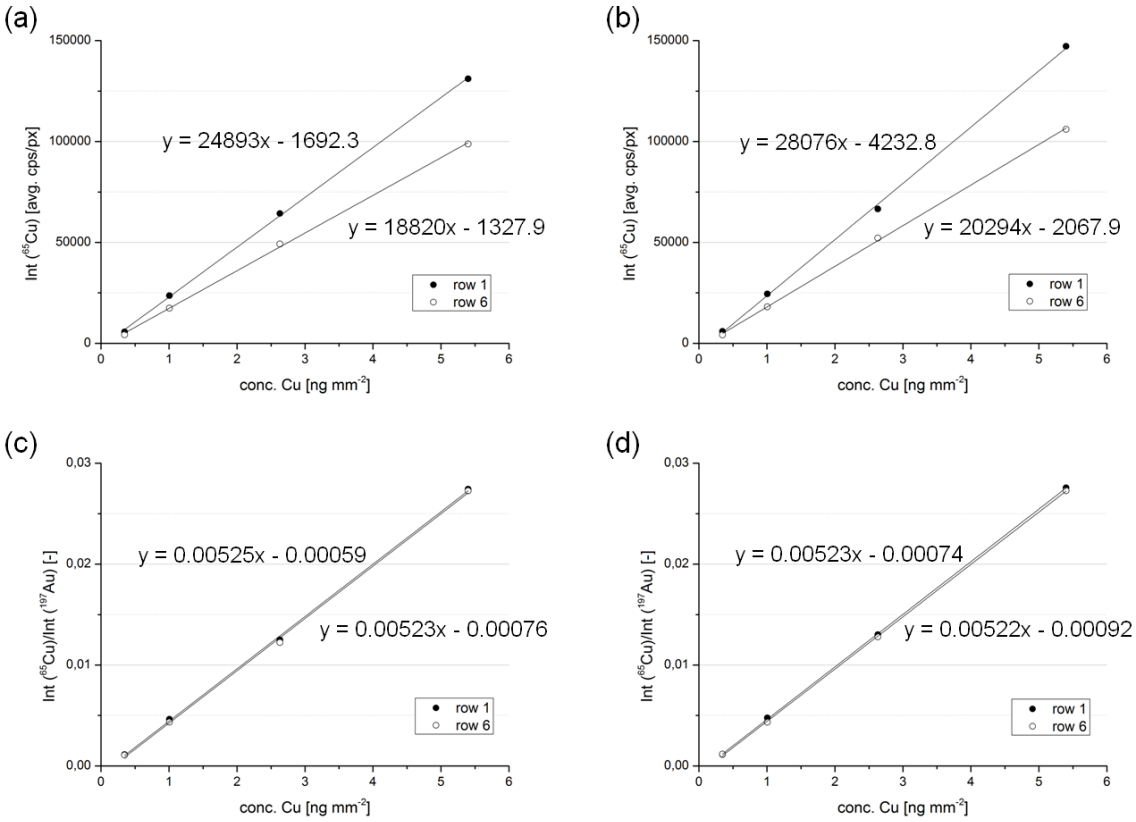

Figure 11: Correlations of the obtained intensity data from the laser ablation experiment and the actual copper concentrations on photo paper (a and c) and transparency foil (b and d) before (a and b) and after (c and d) correction to the gold signal

Comparing the intensity values from single squares underlines the effect of gold standardization. Normalization to the internal standard decreases the RSD of the signal of the printed squares with equal copper concentrations from around 10 to 15% to below 5% for every concentration level. Figure 12 shows this trend graphically. The RSD decreased drastically by gold standardization for every transparency level on the printed pattern. Relative standard deviations of around 5% are low values compared to common laser ablation experiments where RSDs up to 10% are considered as being acceptable.

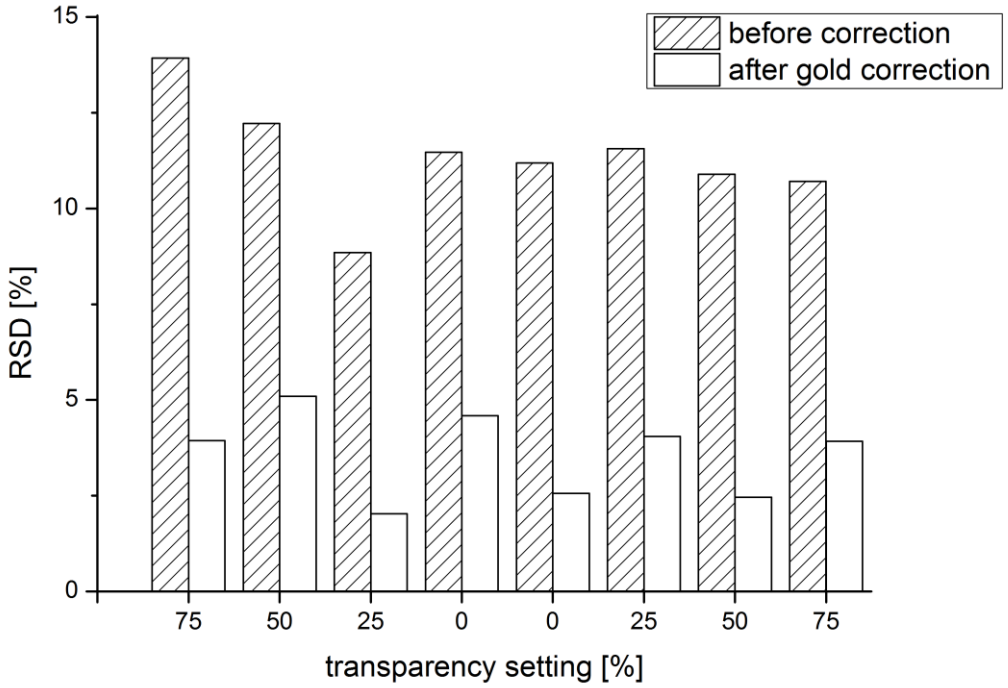

Figure 12: Comparison of the RSD from an average of the six measured replicates of one transparency level before and after gold correction

Improvements in RSD were also observed for equal copper concentrations in one row showing that gold standardization also improves the measurement results without occurring instrumental drifts. Also here the RSD could be lowered significantly to below 5% compared to up to 15% before normalization.

The results underline that gold standardization leads to an improvement of the reliability of the results not only by correcting instrumental drifts during measurement time but also by reducing the standard deviation of the signals within a smaller time scale. This part of the experiment confirms the observations made by Konz *et al.*[33] that gold standardization leads to an enhanced image quality.

Instrumental drifts effect not only the measurement of target analytes but also present matrix elements will show altered signal intensities. The used matrices transparency foil and photo paper mainly consist of carbon and thus it should be evenly distributed over the sample. Figure 13 presents the distribution of ^{13}C before (Figure 13a) and after (Figure 13b) gold standardization.

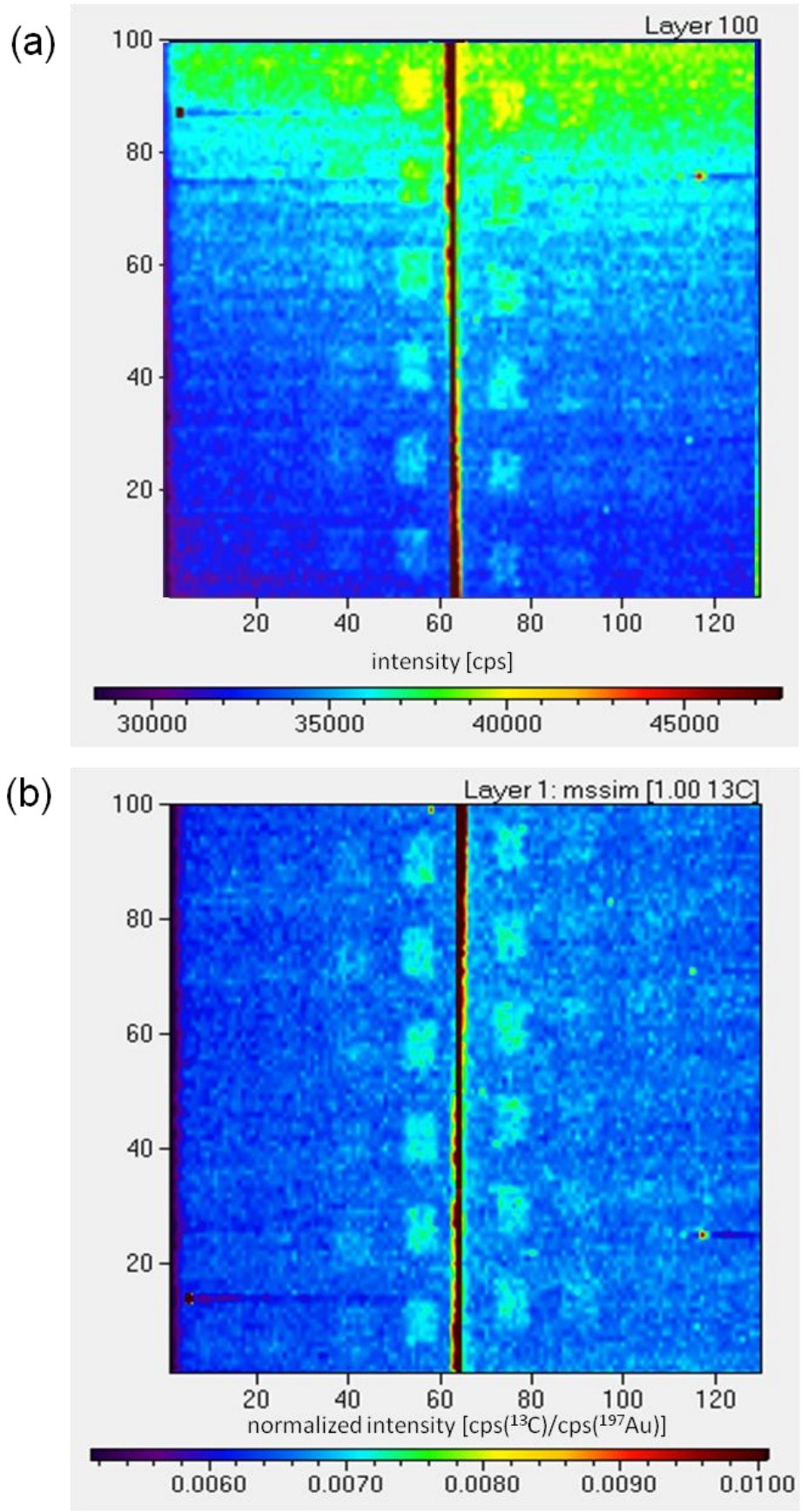

Figure 13: Distribution of ^{13}C before (a) and after (b) gold standardization

Like in the image of the ^{65}Cu distribution the start of the measurement was in the left upper corner of the images. In the uncorrected carbon distribution image a decrease in signal intensity from the beginning to the end of the measurement can be stated. Again, this can be contributed to instrumental drifts. After gold standardization the carbon signal is evenly distributed over the whole sample surface. Square-shaped areas with slightly increasing carbon signal can be explained by the application of the printed patterns. On areas with high amounts of applied ink the carbon signal increases due to a major part of organic components in the ink.

4.3.2 Correction of matrix effects

The ablation process is influenced by the matrix; due to changing material properties differences in the ablation behavior are expected.

Therefore differences in absolute signal intensities of equal analyte concentrations on different sample types are possible. The used internal standard should compensate for these signal changes. The effects of changing matrices was investigated using the print patterns described earlier.

Figure 14a represents the signal intensities on photo paper and on transparency foil in the first row plotted against the actual copper concentrations with a straight-line regression. The slopes of the regressions calculated using the uncorrected intesities differ more than 10% for transparency foil and photo paper indicating differences in the ablation behavior of transparency foil and photo paper. The important factors for the changing signals are differences in the ablation process and variations in the size and shape of the formed aerosol paricles leading to a changed transport into the plasma. These changes are corrected by gold standardization (Figure 14b); resulting differences of the slopes were around 2-4% being within the RSD of replicate measurements on one matrix. Results derived from the other rows confirm the observations.

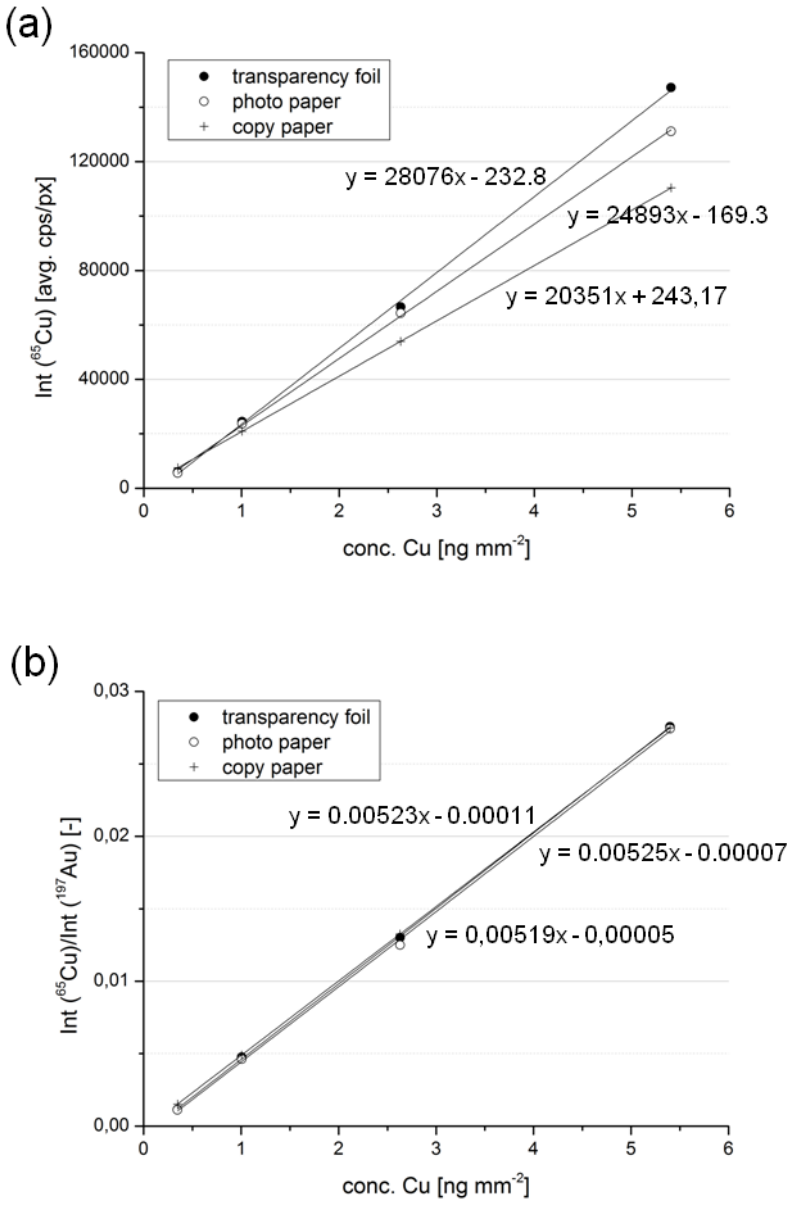

Figure 14: Correlations of the intensity data obtained from the laser ablation experiment with the actual copper concentrations comparing the effects of changing matrices before (a) and after (b) gold standardization. Additionally to the calibrations on photo paper and transparency foil a printed pattern on copy paper was measured to confirm the validity of the calibration

To verify that the developed standardization method is also valid on other materials a pattern similar to the one used in the previous experiment was printed on normal copy paper. Copy paper was chosen as an additional matrix to underline the consequence of matrix effects on the absolute signal intensity and the effectivity of normalization. The four squares with varying concentrations corresponding to the different copper concentrations were printed in five replicates. Actual copper concentration was determined using solution nebulization ICP-MS performing the same procedure as

described earlier. The copper concentrations on copy paper did not differ significantly from those on photo paper and transparency foil confirming that the amount of deposited ink does not depend on the material.

The measurement conditions were the same as employed in the previously presented experiment. Using the raw intensities and the normalized intensities from the imaging experiment again a straight-line regression could be calculated. Compared to the data obtained for photo paper and transparency foil the uncorrected intensities from the image on copy paper differ significantly as presented in Figure 14a. The slope of the regression line on copy paper is approx. 20% beneath the one for photo paper. After correction to the internal standard the slopes of the regression lines seem to be identical with only minor variances (Figure 14b) again showing an RSD being within the range of the measurement uncertainty. The fact that the slope of copy paper is smaller than on photo paper can be affiliated with the ablation behavior of copy paper which tends to create larger pieces when ablated by the laser. The transport efficiency for these particles is rather weak: Therefore less material will be transported into plasma and this will lead to a reduction in overall signal intensity. The phenomenon of particles that will not reach the plasma source could be confirmed by another observation: when the tubing transporting the aerosol to the ICP-MS was disassembled after a few experiments remaining sample material could be found in the tubes. However, as the applied gold layer is also affected by the weaker transport efficiency of ablated copy paper normalization can compensate for this effect.

4.3.3 Correction of day-to-day variations

Besides the correction of changing parameters within one single experiment also the day-to-day comparability of measured values is an important factor. An optimal internal standard should yield comparable normalized intensity results even if the actual intensities differ significantly due to varying instrumental conditions such as vacuum pressure, gas flows and instrumental parameters like torch position, constitution of cones, lens voltages and more.

The stability of the normalized intensity signal for copper was tested using a printed pattern with equal concentrations of copper prepared and measured on different days. Five samples with twelve 400-µm-squares each with a transparency setting of 0% printed on transparency foil were used for this study. The means of the signals for all measured squares in one experiment were compared with and without gold

standardization. Results are graphically presented in Figure 15 showing that the differences between the absolute signal intensities for ^{65}Cu were tremendous. Lowest to highest value differed more than 100%. In contrast to the absolute values the normalized intensities showed only small differences with an RSD below 5% (n = 5). The result indicates that gold normalization is not only suitable for compensation of changes during one measurement but also makes data acquired in independent experiments comparable. The mentioned observations were also made for other matrices (copy and photo paper).

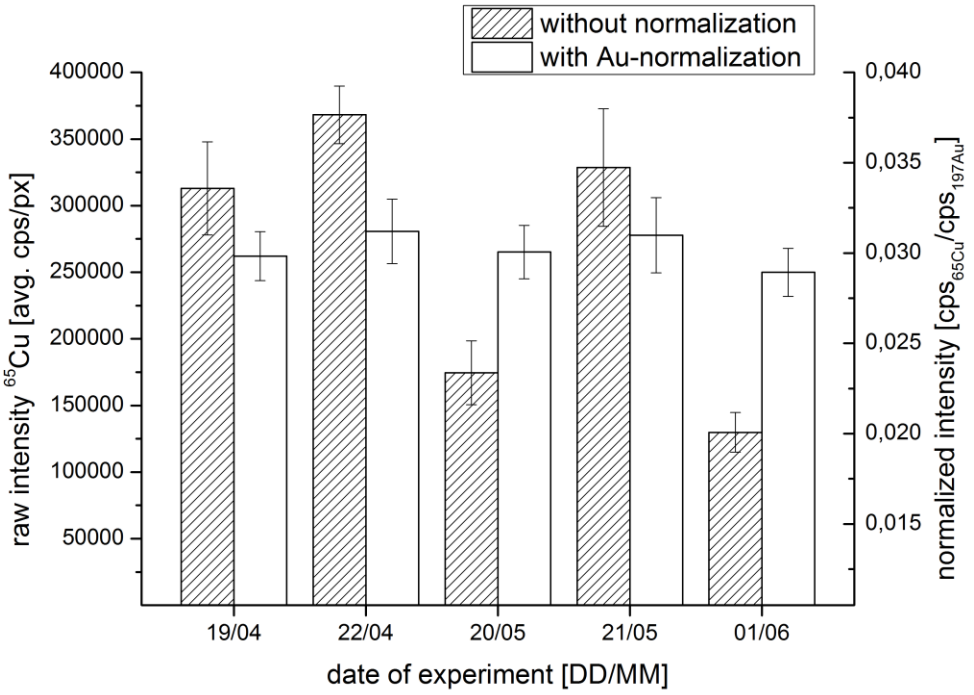

Figure 15: Day-to-day variation of signal intensities with and without gold normalization in five imaging experiments

4.3.4 Carbon as internal standard

Using the performed experiment the suitability of carbon as internal standard could not be evaluated in terms of compensation of matrix effects as the sample material had not been completely ablated. Only the upper layers containing copper were ablated, so no quantitative statement about the ablated carbon can be made. However, if carbon was a suitable internals standard it should still compensate for instrumental drifts. Here the considerations are made for only one matrix each and so the results are independent from ablation differences. The results show that normalization reduced the effect of the instrumental drift and the difference of the slope from the first to the last row on one

matrix could be reduced from 25% to about 10%. Figure 16 shows the regression lines for copper after normalization to the carbon signal. Still a difference in the slopes remains and the instrumental drift could not be completely compensated.

Only the results for transparency foil as matrix are shown here; the same observations were made for the values on photo paper.

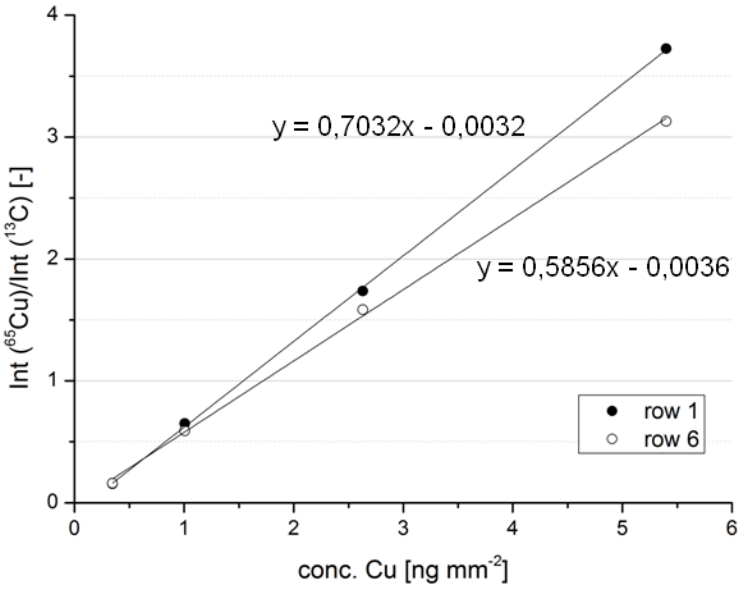

Figure 16: Regression of the intensity values in first and last row on transparency foil corrected to the carbon signal

Alone these results exclude carbon from the list of suitable internal standards when even instrumental drifts cannot be compensated. The fact that the carbon signal decreases in a different way than the copper signal may be traced back to changing plasma conditions during the measurement. When the plasma temperature only slightly changes the ionization efficiency of carbon will be more affected than the one of metallic analytes due to the high first ionization potential of carbon.

4.4 Imaging experiments

With the gained knowledge that gold standardization compensates for sample dependent and instrumental changes during one experiment as well as for changes in signal intensities on different measurement days the proposed approach could be utilized for quantification of copper in LA-ICP-MS images of unknown samples. Having shown that this procedure is valid on materials such as copy paper, photo paper and

transparency foil it will also be applicable to a number of unknown samples with similar composition.

4.4.1 Imaging of copper on a post stamp

In a final application example a post stamp with blue coloring containing copper was chosen for analysis. An area with the size of 3 x 12 mm on the stamp was selected for imaging. Special care was taken to quantitatively ablate the sample material to obtain reliable information about the actual amount of copper; again the measurement conditions were kept constant to the previous experiments. Acquisition time was approx. 4 h. Complete ablation of the copper containing ink was proven by a second ablation round over the sample where the signal for copper did not exceed the background level. The resulting distribution image is shown in Figure 17 additional to a visual image of the stamp with an enlarged view of the analyzed area. The generated image was 60 x 240 pixels in size with a spatial resolution of 50 µm in both vertical and horizontal direction.

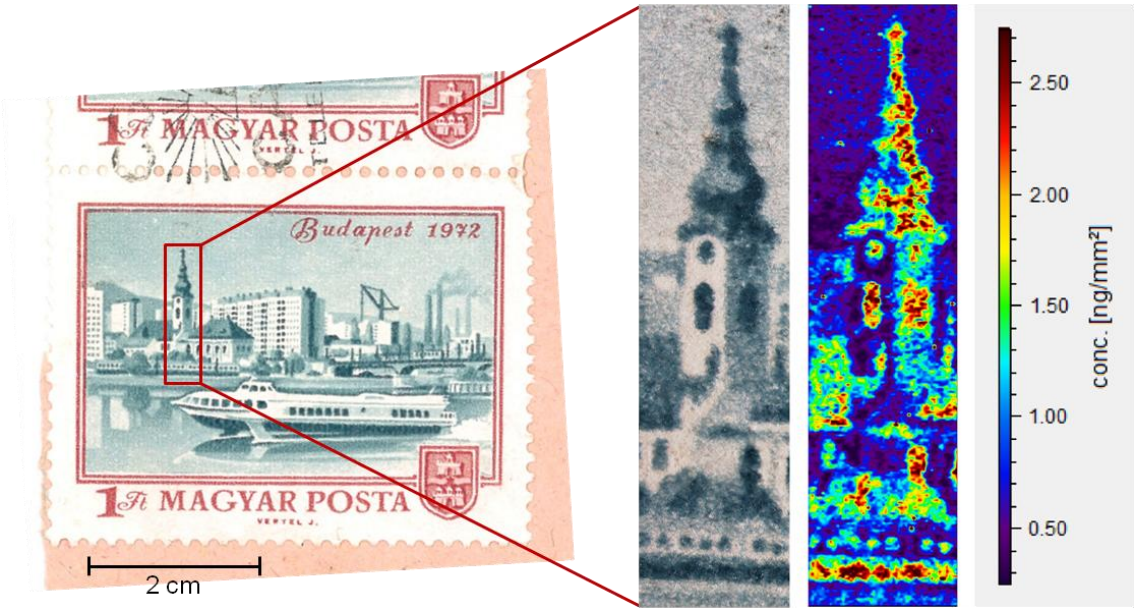

Figure 17: Visual image of the post stamp used for the imaging with an enlarged view of the area of interest and the generated distribution image with calculated copper concentrations (from left to right)

Quantification of the derived signals was based on the calibration obtained from the measurements on photo paper and transparency foil presented before. The resulting image for the copper distribution clearly represents the graphic shown within the analyzed area. Concentration variations could be illustrated in the distribution image whereby sections with visibly darker coloring contain more copper than ones appearing

in lighter blue. Sample details like the clock and the window on the steeple could be depicted as well as further details such as trees and bushes. Even smaller structures like the chaplet-like structure at the bottom of the image could be displayed. Different lighting conditions as on the top of the steeple were illustrated resulting in different detected copper concentrations. Also the shape of the top of the steeple is represented by the copper distribution. Summing up the distribution image for copper shows high accordance with the micrograph taken before the laser ablation experiment not only by means of qualitative consensus but also representing the different shades of the blue coloring.

Commonly used intensity plots offer only qualitative information about the distribution of the analyte within the sample. In this experiment real concentrations based on a reliable calibration together with solid internal quantification can be presented.

4.4.2 Imaging of copper in a modified petal

The blossom of a white peony (*Paeonia officinalis*) was allowed to incorporate blue pen ink (Pelikan type 4001, diluted 1:1 v/v with tap water) through the stalk for a period of 5 h. Selected petals were removed and completely dried. Optically the blue color was enriched in the petal's veins especially in the outer regions of the petals. Pieces of the plant tissue were cut and attached to a glass slide using double sided tape. Defined areas of the dried petals were cut and after calculation of the area their mass was determined to create a calibration scale for micrograms copper per gram dry weight [µg g^{-1}]. After gold coating an area of the sample was ablated using laser parameters leading to complete ablation of the material. A laser energy of 45% at 10 Hz repetition rate with 50 µm laser beam diameter and 50 µm s^{-1} scan speed was employed for the described experiment. From the resulting time resolved intensity plots for the measured isotopes elemental images could be calculated. The measured isotopes were ^{13}C, ^{63}Cu, ^{65}Cu and ^{197}Au as in the previous experiments.

Figure 18 shows the distribution of copper and a microscopic image of the analyzed area which is 6 x 6 mm in size. The resulting elemental image has a spatial resolution of 50 µm in horizontal and vertical direction. As the blue color indicates copper seems to appear in higher concentrations in the veins. Detailed structures could be depicted using the applied laser beam diameter. The distribution of copper shows that copper is not only present on areas with blue color. Whereas the blue stain seems to be accumulated in the outer areas of the petal copper is enriched in the veins throughout the chosen

sample. The copper concentration seems to be especially enriched in some veins such as the structure on the right side of the image. Lighter areas on the petal are appearing in the micrograph. Also these structures could be depicted having a smaller copper concentration. Again, the regression from the paper-foil model was used for quantification of the derived analyte signals. As the complete sample material has been ablated during the laser ablation experiment the detected amount of copper can be directly affiliated with a concentration.

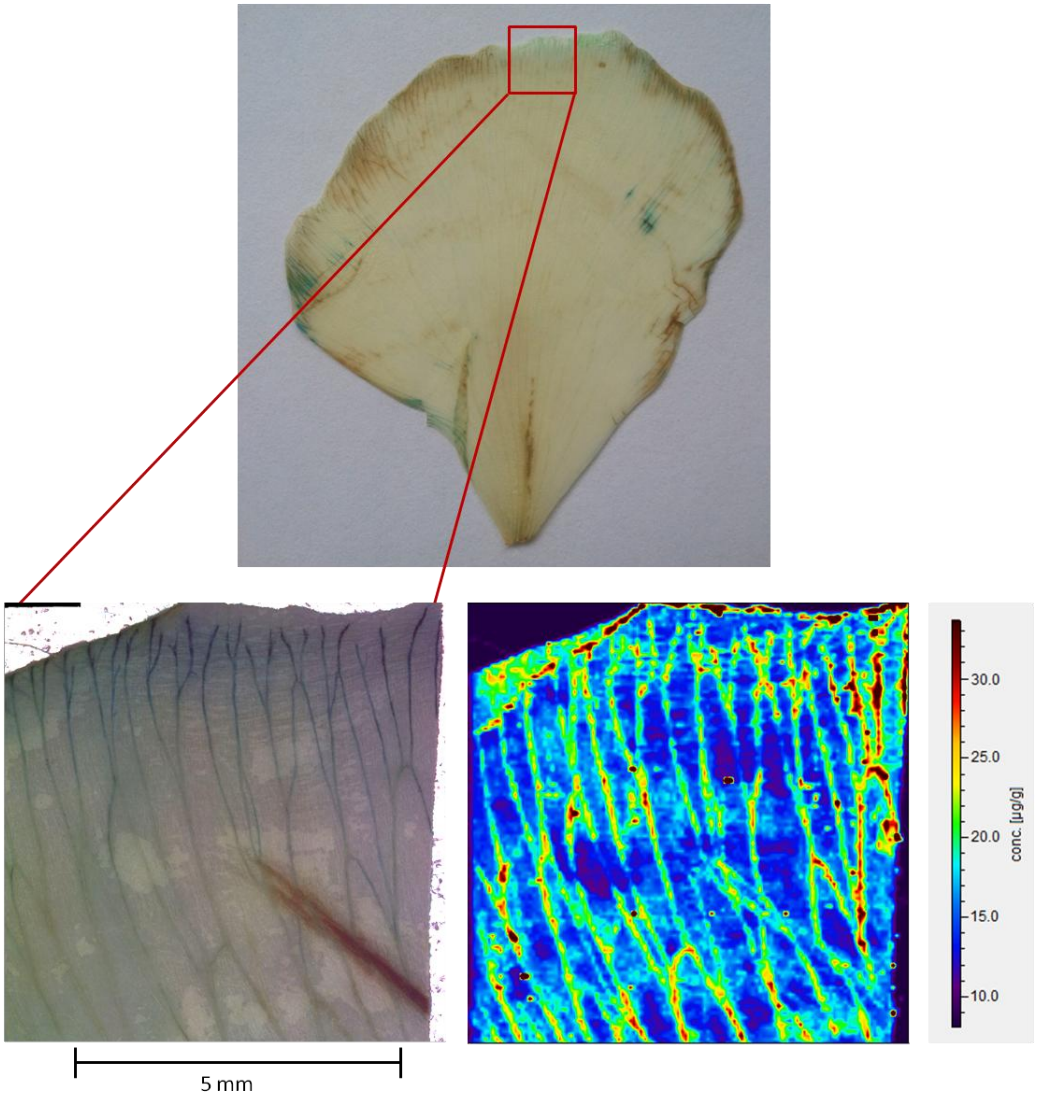

Figure 18: A dried peony petal spiked with copper containing pen ink; overview image of the petal (left), microscopic image of the analyzed area (middle) and copper distribution (^{65}Cu) with concentrations in ng g-1 (right)

5. Conclusion

The compensation of instrumental drifts is highly important due the very long acquisition times for imaging experiments up to many hours. Matrix effects have to be compensated as biological materials are often highly inhomogeneous and slight changes in the material properties may lead to differences in the recorded absolute signal intensity for the chosen analytes due to changed ablation behavior of the alternating tissue.

During the performed experiments the suitability of gold thin-layers as internal standards for LA-ICP-MS imaging experiments has been evaluated. Diverse organic materials such as transparency foil or various paper types in combination with printed inkjet patterns have been considered being a suitable alternative for tissue sections for reliable method development. Reproducibility of the created print patterns is an important factor favoring the artificial samples to tissue slices as method development is much easier when sample alterations do not have to be taken into consideration.

In the presented work gold has been shown to be a reliable internal standard for imaging experiments on samples being similar to biological samples in terms of material properties such as density and carbon content. It could be demonstrated that gold standardization allows for the compensation of instrumental drifts during measurement time as well as for the reduction of matrix related signal differences originating from ablation differences and other matrix effects. Additionally, gold normalization makes the comparison of experiments carried out on different days more reliable. Day-to-day comparability of measurements also makes quantification much easier as not for every new experiment a new standard has to be prepared and measured which makes imaging experiments more time efficient. The work shows that gold standardization contributes to the improvement of qualitative information of LA-ICP-MS imaging experiments and furthermore allows reliable quantitative predication of analyte distributions. The used print patterns are a promising approach for reliable and easy quantification of a large scale of elements in LA-ICP-MS imaging experiments on biological samples.

Thus, gold standardization is a helpful tool to make the qualitative results of imaging experiments more confidable and supports the reliability of quantitative imaging experiments. The developed method could be transferred from artificially created materials to unknown samples. The validity of the quantification method has been proved using a printed pattern on copy paper with known amounts of copper. It showed

that the patterns on other materials yielded normalized intensity values being comparable to this sample showing that gold standardization compensates for matrix relates signal differences. The established method could be applied on samples with unknown amounts of copper after this proof of principle. Quantitative results for the elemental concentrations on the samples were obtained using standards printed on transparency foils and photo paper for the estimation of the copper content. The method has not only been transferred to a paper sample with unknown copper amounts in form of a post stamp but also to a biological sample being a peony petal spiked with copper from blue ink for visualization of the copper uptake of the plant. The elemental distributions for both samples delivered excellent correlations with the optical images and the expected copper distributions. Quantitative estimations of the copper content are considered being of high accuracy due to the applied gold standardization which compensates for multiple changes in signal intensity.

Further improvements of the method include an expansion of the range of elements available for quantification and improving the spatial resolution of the obtained images.

6. Outlook

The presented work offers a lot of satisfactory results showing that further experiments might lead to tremendous improvements within the field of quantitative LA-ICP-MS imaging on biological samples. Reliable quantification in this field of science has often not been given the maximum attention and with the proposed approach lots of improvements have been made.

During this work the quantification procedure has only been developed for copper. However, many other metallic as well as non metallic elements are of great interest in the field of life sciences. Therefore the established method has to be implemented for a larger variety of elements to give access to a greater range of reliably quantifiable elements being of interest for biological and biomedical questions. The approach to employ printed patterns as external standard for imaging experiments is considered being an easy and straightforward method that can also be made accessible for other elements. It is possible to add elemental spikes to the cartridges of commercially available office inkjet printers. By this way any element can be chosen for printing on an inkjet pattern; it is even possible to perform multi-elemental calibrations in one inkjet pattern by using multi-elemental spike solutions. Apart from the use of normal office inkjet printers it is also possible to employ printers especially designed for scientific purposes. Using those instrumentations it is possible to make almost any solution available for accurate inkjet printing. Multi-elemental standard solutions could be printed to transparency foil or paper without prior modifications or only after addition of a pigment or dye to make the printed patterns visible. This would be a more sophisticated approach than the office inkjet printer used during the presented experiments. Further work will be directed on the overall improvement of the quantification method for making the obtained results even more reliable. Different other matrices should be tested to verify that the compensation for matrix effects is valid for a larger number of materials.

Improving the spatial resolution of the obtained images is also of great importance. For special applications a resolution of 50 µm/pixel may not be satisfactory. The development of measurement procedures making resolutions down to the single cell level accessible is a big goal in the field of laser ablation imaging. Not only the laser parameters need to be tuned for this purpose but also the ICP-MS sensitivities have to reach new maxima to be able to detect smallest amounts of analyte.

In upcoming experiments more attention will be directed to the analysis of biological samples with background of biological or medical interest. Comparisons of the images obtained by LA-ICP-MS with images derived from other elemental or molecular imaging techniques (MALDI, ToF-SIMS, …) are of special interest. Thus, the biological information obtained by the distribution images could even be increased by the synergy of different fields of science. As not only elemental information is of great importance within the field of life sciences obtaining molecular information on the analyte distributions in tissues is of major interest. Complementary imaging techniques could be used – and if non-destructive – even on the same tissue slice to provide not only elemental information but also insight to molecular processes.

Es ist das, was die Toren Zauber nennen und wovon sie meinen, es werde von Dämonen bewirkt. Nichts wird von Dämonen bewirkt, es gibt keine Dämonen. Jeder kann zaubern, jeder kann seine Ziele erreichen, wenn er denken kann, wenn er warten kann […].

Herrmann Hesse, Siddhartha

Figures

Tables

Literature

1. Vanhoe, H., *A review of the capabilities of ICP-MS for trace element analysis in body fluids and tissues.* J Trace Elem Electrolytes Health Dis, 1993. **7**(3): p. 131-9.

2. Mounicou, S., J. Szpunar, and R. Lobinski, *Inductively-coupled plasma mass spectrometry in proteomics, metabolomics and metallomics studies.* Eur J Mass Spectrom (Chichester, Eng), 2010. **16**(3): p. 243-53.

3. Sanz-Medel, A., et al., *ICP-MS for absolute quantification of proteins for heteroatom-tagged, targeted proteomics.* TrAC Trends in Analytical Chemistry, 2012. **40**(0): p. 52-63.

4. Sanz-Medel, A., et al., *Elemental mass spectrometry for quantitative proteomics.* Anal Bioanal Chem, 2008. **390**(1): p. 3-16.

5. Giesen, C., et al., *History of inductively coupled plasma mass spectrometry-based immunoassays.* Spectrochimica Acta Part B: Atomic Spectroscopy, 2012. **76**(0): p. 27-39.

6. del Castillo Busto, M.E., M. Montes-Bayón, and A. Sanz-Medel, *Accurate Determination of Human Serum Transferrin Isoforms: Exploring Metal-Specific Isotope Dilution Analysis as a Quantitative Proteomic Tool.* Anal Chem, 2006. **78**(24): p. 8218-8226.

7. Mokgalaka, N.S. and J.L. Gardea-Torresdey, *Laser Ablation Inductively Coupled Plasma Mass Spectrometry: Principles and Applications.* Applied Spectroscopy Reviews, 2006. **41**(2): p. 131-150.

8. Günther, D. and B. Hattendorf, *Solid sample analysis using laser ablation inductively coupled plasma mass spectrometry.* TrAC Trends in Analytical Chemistry, 2005. **24**(3): p. 255-265.

9. Koch, J. and D. Gunther, *Review of the state-of-the-art of laser ablation inductively coupled plasma mass spectrometry.* Appl Spectrosc, 2011. **65**(5): p. 155-62.

10. Becker, J.S., et al., *Bioimaging of metals by laser ablation inductively coupled plasma mass spectrometry (LA-ICP-MS).* Mass Spectrom Rev, 2010. **29**(1): p. 156-75.

11. Nakanishi, T., et al., *Topologies of amyloidogenic proteins in Congo red-positive sliced sections of formalin-fixed paraffin embedded tissues by MALDI-MS imaging coupled with on-tissue tryptic digestion.* Clin Biochem, 2013.

12. Rompp, A. and B. Spengler, *Mass spectrometry imaging with high resolution in mass and space.* Histochem Cell Biol, 2013. **139**(6): p. 759-83.

13. Desbenoit, N., et al., *Localisation and quantification of benzalkonium chloride in eye tissue by TOF-SIMS imaging and liquid chromatography mass spectrometry.* Anal Bioanal Chem, 2013. **405**(12): p. 4039-49.

14. Piwowar, A.M., et al., *C60-ToF SIMS imaging of frozen hydrated HeLa cells.* Surf Interface Anal, 2013. **45**(1): p. 302-304.

15. Bhargava, R., *Infrared spectroscopic imaging: the next generation.* Appl Spectrosc, 2012. **66**(10): p. 1091-120.

16. Al-Ebraheem, A., M.J. Farquharson, and E. Ryan, *The evaluation of biologically important trace metals in liver, kidney and breast tissue.* Appl Radiat Isot, 2009. **67**(3): p. 470-4.

17. Carvalho, M.L., et al., *Trace elements in human cancerous and healthy tissues: A comparative study by EDXRF, TXRF, synchrotron radiation and PIXE.* Spectrochimica Acta Part B: Atomic Spectroscopy, 2007. **62**(9): p. 1004-1011.

18. Becker, J.S. and N. Jakubowski, *The synergy of elemental and biomolecular mass spectrometry: new analytical strategies in life sciences.* Chem Soc Rev, 2009. **38**(7): p. 1969-83.

19. Becker, J.S., et al., *Bioimaging of Metals and Biomolecules in Mouse Heart by Laser Ablation Inductively Coupled Plasma Mass Spectrometry and Secondary Ion Mass Spectrometry.* Anal Chem, 2010. **82**(22): p. 9528-9533.

20. Wang, L.M., et al., *Bioimaging of copper alterations in the aging mouse brain by autoradiography, laser ablation inductively coupled plasma mass spectrometry and immunohistochemistry.* Metallomics, 2010. **2**(5): p. 348-53.

21. Becker, J.S., et al., *Bioimaging of metals in brain tissue by laser ablation inductively coupled plasma mass spectrometry (LA-ICP-MS) and metallomics.* Metallomics, 2010. **2**(2): p. 104-11.

22. Hare, D., et al., *Elemental bio-imaging of melanoma in lymph node biopsies.* Analyst, 2009. **134**(3): p. 450-3.

23. M-M, P., et al., *Novel bioimaging techniques of metals by laser ablation inductively coupled plasma mass spectrometry for diagnosis of fibrotic and cirrhotic liver disorders.* PLoS One, 2013. **8**(3): p. e58702.

24. Bourassa, M.W. and L.M. Miller, *Metal imaging in neurodegenerative diseases.* Metallomics, 2012. **4**(8): p. 721-38.

25. da Silva, M.A. and M.A. Arruda, *Laser ablation (imaging) for mapping and determining Se and S in sunflower leaves.* Metallomics, 2013. **5**(1): p. 62-7.

26. Austin, C., et al., *Elemental bio-imaging of calcium phosphate crystal deposits in knee samples from arthritic patients.* Metallomics, 2009. **1**(2): p. 142-7.

27. Dressler, V.L., et al., *Biomonitoring of essential and toxic metals in single hair using on-line solution-based calibration in laser ablation inductively coupled plasma mass spectrometry.* Talanta, 2010. **82**(5): p. 1770-7.

28. Sela, H., et al., *Biomonitoring of hair samples by laser ablation inductively coupled plasma mass spectrometry (LA-ICP-MS).* International Journal of Mass Spectrometry, 2007. **261**(2–3): p. 199-207.

29. Moreno-Gordaliza, E., et al., *Elemental bioimaging in kidney by LA-ICP-MS as a tool to study nephrotoxicity and renal protective strategies in cisplatin therapies.* Anal Chem, 2011. **83**(20): p. 7933-40.

30. Gholap, D., et al., *Use of pneumatic nebulization and laser ablation-inductively coupled plasma-mass spectrometry to study the distribution and bioavailability of an intraperitoneally administered Pt-containing chemotherapeutic drug.* Anal Bioanal Chem, 2012. **402**(6): p. 2121-9.

31. Austin, C., et al., *Factors affecting internal standard selection for quantitative elemental bio-imaging of soft tissues by LA-ICP-MS.* Journal of Analytical Atomic Spectrometry, 2011. **26**(7): p. 1494-1501.

32. Frick, D.A. and D. Gunther, *Fundamental studies on the ablation behaviour of carbon in LA-ICP-MS with respect to the suitability as internal standard.* Journal of Analytical Atomic Spectrometry, 2012. **27**(8): p. 1294-1303.

33. Konz, I., et al., *Gold internal standard correction for elemental imaging of soft tissue sections by LA-ICP-MS: element distribution in eye microstructures.* Anal Bioanal Chem, 2013. **405**(10): p. 3091-6.

34. Maiman, T.H., *Stimulated Optical Radiation in Ruby.* Nature, 1960. **187**(4736): p. 493-494.

35. Thompson, M., J.E. Goulter, and F. Sieper, *Laser ablation for the introduction of solid samples into an inductively coupled plasma for atomic-emission spectrometry.* Analyst, 1981. **106**(1258): p. 32-39.

36. Gray, A.L., *Solid sample introduction by laser ablation for inductively coupled plasma source mass spectrometry.* Analyst, 1985. **110**(5): p. 551-556.

37. Zaichick, S. and V. Zaichick, *Trace elements of normal, benign hypertrophic and cancerous tissues of the human prostate gland investigated by neutron activation analysis.* Appl Radiat Isot, 2012. **70**(1): p. 81-7.

38. Becker, J.S., et al., *Bioimaging of metals and biomolecules in mouse heart by laser ablation inductively coupled plasma mass spectrometry and secondary ion mass spectrometry.* Anal Chem, 2010. **82**(22): p. 9528-33.

39. Becker, J.S., *Imaging of metals, metalloids, and non-metals by laser ablation inductively coupled plasma mass spectrometry (LA-ICP-MS) in biological tissues.* Methods Mol Biol, 2010. **656**: p. 51-82.

40. Berg, D., et al., *Use of formalin-fixed and paraffin-embedded tissues for diagnosis and therapy in routine clinical settings.* Methods Mol Biol, 2011. **785**: p. 109-22.

41. Lear, J., et al., *Improving acquisition times of elemental bio-imaging for quadrupole-based LA-ICP-MS.* Journal of Analytical Atomic Spectrometry, 2012. **27**(1): p. 159-164.

42. Heymsfield, S.B., et al., *Chemical and elemental analysis of humans in vivo using improved body composition models.* Am J Physiol, 1991. **261**(2 Pt 1): p. E190-8.

43. Berman, H.M., et al., *The Protein Data Bank.* Nucleic Acids Res, 2000. **28**(1): p. 235-42.

44. Sychrova, H., *Yeast as a model organism to study transport and homeostasis of alkali metal cations.* Physiol Res, 2004. **53 Suppl 1**: p. S91-8.

45. Levitan, I.B., *Modulation of ion channels in neurons and other cells.* Annu Rev Neurosci, 1988. **11**: p. 119-36.

46. Mahan, D.C. and R.G. Shields, Jr., *Macro- and micromineral composition of pigs from birth to 145 kilograms of body weight.* J Anim Sci, 1998. **76**(2): p. 506-12.

47. Lill, R., *Function and biogenesis of iron-sulphur proteins.* Nature, 2009. **460**(7257): p. 831-8.

48. Fontecilla-Camps, J.C., et al., *Structure-function relationships of anaerobic gas-processing metalloenzymes.* Nature, 2009. **460**(7257): p. 814-22.

49. Schwarz, G., R.R. Mendel, and M.W. Ribbe, *Molybdenum cofactors, enzymes and pathways.* Nature, 2009. **460**(7257): p. 839-47.

50. Todd, R.C. and S.J. Lippard, *Inhibition of transcription by platinum antitumor compounds.* Metallomics, 2009. **1**(4): p. 280-291.